INTERNATIONAL ATOMIC ENERGY AGENCY
UNITED NATIONS EDUCATIONAL, SCIENTIFIC AND CULTURAL ORGANIZATION
INTERNATIONAL CENTRE FOR THEORETICAL PHYSICS
I.C.T.P., P.O. BOX [illegible], 34100 TRIESTE, ITALY, CABLE: CENTRATOM TRIESTE

H4.SMR/449-25

WINTER COLLEGE ON HIGH RESOLUTION SPECTROSCOPY

(8 January - 2 February 1990)

COHERENT TRAPPING IN LASER COOLING

E. Arimondo

Università di Pisa
Dipartimento di Fisica
Pisa 56100
Italy

Laser Cooling below the One-Photon Recoil Energy by Velocity-Selective Coherent Population Trapping

A. Aspect, E. Arimondo,[a] R. Kaiser, N. Vansteenkiste, and C. Cohen-Tannoudji

Laboratoire de Spectroscopie Hertzienne de l'Ecole Normale Supérieure et Collège de France, F-75231 Paris Cedex 05, France

(Received 11 July 1988)

We present a new laser-cooling scheme based on velocity-selective optical pumping of atoms into a nonabsorbing coherent superposition of states. This method has allowed us to achieve transverse cooling of metastable ^{4}He atoms to a temperature of 2 μK, lower than both the usual Doppler cooling limit (23 μK) and the one-photon recoil energy (4 μK). The corresponding de Broglie wavelength (1.4 μm) is larger than the atomic-transition optical wavelength.

PACS numbers: 32.80.Pj, 42.50.Vk

The lowest temperature T which can be achieved by the usual laser-Doppler-cooling method is given, for a two-level atom, by $k_B T/2 = \hbar\Gamma/4$, where Γ is the spontaneous-emission rate from the excited atomic state (for Na, $T = 240$ μK).[1] In order to reach lower temperatures, proposals based on Raman two-photon processes in a three-level atom have been presented,[2,3] but the efficiency of Raman cooling has not yet been demonstrated. Recently, surprisingly low temperatures (around 40 μK) have been measured for sodium[4] and tentatively interpreted in terms of a new friction mechanism.[5] The recoil energy $(\hbar k)^2/2M$ for an atom with mass M emitting a photon with momentum $\hbar\mathbf{k}$ represents another landmark in the energy scale for laser cooling. It has been suggested that optical pumping in translation space might be used to cool the translational degrees of freedom below this so-called recoil limit, by velocity-selective recycling in a trap.[6] In this Letter, we present a mechanism of laser cooling below the one-photon recoil energy, based on optical pumping of both internal and translational atomic degrees of freedom. This velocity-selective process is based on coherent trapping of atomic populations[7] and has allowed us to achieve a one-dimensional cooling of ^{4}He atoms in the triplet metastable state down to a temperature of about 2 μK. This temperature is lower than both the Doppler cooling limit (23 μK for 1D cooling) and the one-photon recoil energy (4 μK).

Our scheme involves a closed three-level Λ configuration where two degenerate ground Zeeman sublevels $g_\pm$ ($m = \pm 1$) are coupled to an excited level e_0 ($m = 0$) by two counterpropagating σ_+ and σ_- laser beams with the same frequency ω_L and the same intensity (solid lines of Fig. 1). For an atom at rest, two-photon Raman processes give rise to a nonabsorbing coherent superposition of g_+ and g_-. If the atom is moving along $0z$, the Raman resonance condition is no longer fulfilled as a consequence of opposite Doppler shifts on the two counterpropagating laser beams. This simple argument explains how the phenomenon of coherent population trapping can be velocity selective for appropriate laser configurations.[8] Our cooling scheme consists of accumulating atoms in the zero-velocity nonabsorbing state where they remain trapped. To populate this state, we take advantage of momentum redistribution due to spontaneous emission, which allows certain atoms to be optically pumped from the absorbing velocity classes to the nonabsorbing state. Since the recoil of the last spontaneous-emission photon is part of the cooling mechanism, the one-photon recoil energy is not a limit and the final temperature is limited only by the coherent interaction time. Note also that, contrary to other cooling schemes, our mechanism, based on a Raman resonance condition, does not depend on the sign of the laser detuning.

A more rigorous analysis requires the introduction of both internal and translational quantum numbers. For example, the state $|e_0,p\rangle$ represents an atom in level e_0 with the value p of P_z^{at} ($\mathbf{P}^{at}$ is the atomic momentum). If we ignore spontaneous emission, $|e_0,p\rangle$ is coupled only to $|g_-,p-\hbar k\rangle$ (or $|g_+,p+\hbar k\rangle$) by stimulated emission of a σ_+ (σ_-) laser photon carrying a momentum

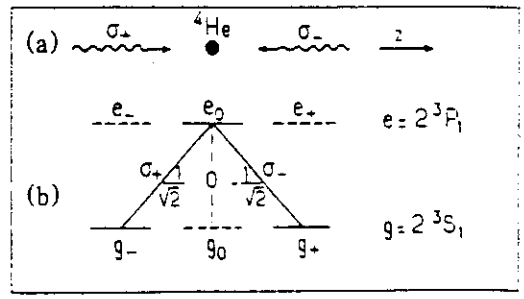

FIG. 1. (a) Two counterpropagating σ_+ and σ_- polarized laser beams interact with ^{4}He atoms on the 2^3S_1-2^3P_1 transition. (b) The Zeeman sublevels, and some useful Clebsch-Gordan coefficients. Since the $e_0 \rightarrow g_0$ transition is forbidden, all atoms are pumped into g_+ and g_- after a few fluorescence cycles. These two levels are coupled only to e_0, and a closed three-level Λ configuration is realized (solid lines).

$+\hbar k$ ($-\hbar k$). We are thus led to introduce, for each value of p, a family $F(p)$ of three states $\{|e_0,p\rangle, |g_+,p+\hbar k\rangle$, and $|g_-,p-\hbar k\rangle\}$ which are coupled by the interaction Hamiltonian V (Ref. 9):

$$\langle g_\pm,p\pm\hbar k|V|e_0,p\rangle = \mp(\hbar\omega_1/2)\exp(i\omega_L t),$$

where ω_1 is the Rabi frequency associated with each laser and where the $\mp$ signs come from the Clebsch-Gordan coefficients $e_0 \leftrightarrow g_+$ and $e_0 \leftrightarrow g_-$ (Fig. 1). Note that for $p \neq 0$, the kinetic energy $(p+\hbar k)^2/2M$ of $|g_+,p+\hbar k\rangle$ differs from the kinetic energy $(p-\hbar k)^2/2M$ of $|g_-,p-\hbar k\rangle$ by an amount $2\hbar kp/M$ (i.e., the Doppler shift introduced above for the two-photon Raman resonance).

We can now write the expression of the nonabsorbing trapping state considered above:

$$|\psi_{NA}(0)\rangle = [|g_-,-\hbar k\rangle + |g_+,+\hbar k\rangle]/\sqrt{2}.$$

This state is stationary since the two states $|g_\pm,\pm\hbar k\rangle$ have the same internal and kinetic energies, and since $\langle\psi_{NA}(0)|V|e_0,0\rangle = 0$. These properties are not modified when spontaneous emission is taken into account [$|\psi_{NA}(0)\rangle$ is radiatively stable], so that an atom pumped in this state remains trapped there indefinitely (coherent population trapping). Note that $|\psi_{NA}(0)\rangle$ is not an eigenstate of P_z^{at}, so that, for atoms trapped in $|\psi_{NA}(0)\rangle$, the atomic momentum distribution presents two peaks at eigenvalues $p_{at} = \pm\hbar k$.

For the families $F(p\neq 0)$, we can introduce two orthogonal linear combinations of $|g_\pm,p\pm\hbar k\rangle$:

$$|\psi_{NA}(p)\rangle = [|g_-,p-\hbar k\rangle + |g_+,p+\hbar k\rangle]/\sqrt{2},$$

$$|\psi_A(p)\rangle = [|g_-,p-\hbar k\rangle - |g_+,p+\hbar k\rangle]/\sqrt{2}.$$

The first one, $|\psi_{NA}(p)\rangle$, is not coupled to $|e_0,p\rangle$, while $|\psi_A(p)\rangle$ is coupled to $|e_0,p\rangle$ with a Rabi frequency $\sqrt{2}\omega_1$. However, the nonabsorbing state $|\psi_{NA}(p)\rangle$ is not a trapping state, because it is not stationary (the energies of $|g_\pm,p\pm\hbar k\rangle$ differ by $2\hbar kp/M$). More precisely, if an atom is in $|\psi_{NA}(p)\rangle$ at $t=0$, it will oscillate between $|\psi_{NA}(p)\rangle$ and the absorbing state $|\psi_A(p)\rangle$ at the frequency $2kp/M$. One can then show that for small values of p [$kp/M \ll \Gamma'$ where $\Gamma' = \omega_1^2/\Gamma$ is the absorption rate from $|\psi_A(p)\rangle$ for $\omega_1 \ll \Gamma$ and zero detuning], the absorption rate from $|\psi_{NA}(p)\rangle$ is of the order of $\Gamma'' = (kp/M)^2/\Gamma'$. The smaller p, the longer the time spent in $|\psi_{NA}(p)\rangle$. We have thus achieved a velocity-selective coherent population trapping.[10]

So far, we have only considered the evolution of a given p family. Spontaneous emission can actually redistribute atoms between different families since the one-photon recoil momentum along $0z$ due to such a process is a random variable between $-\hbar k$ and $+\hbar k$. Such a random walk in momentum space is essential for the cooling discussed here. It provides the mechanism for the pumping and accumulation of atoms into the nonabsorbing superposition of states $|\psi_{NA}(p)\rangle$ with $p=0$ or very small. The longer the interaction time Θ, the narrower the range $\pm\delta p$ of values of p around $p=0$ for the states $|\psi_{NA}(p)\rangle$ in which the atoms can remain trapped during Θ, and the greater the number of fluorescence cycles which can bring them into these states. For Θ large enough so that $\delta p \leq \hbar k$, the final atomic momentum distribution $\mathcal{P}(p_{at})$ along $0z$ will exhibit two resolved peaks emerging at $\pm\hbar k$ above the initial distribution. This will be the signature of cooling by velocity-selective coherent trapping.

We have performed a quantitative calculation of such a "generalized optical pumping cycle" (in both internal and momentum spaces) which confirms all the previous predictions. Such a calculation is based on three-level generalized optical Bloch equations involving internal and external degrees of freedom.[11] Because of spontaneous emission, these equations are finite-difference equations. It must be emphasized that, since the width δp can become smaller than $\hbar k$, most of the standard approximation methods used in laser-cooling theories[1-8] break down: Especially, it is no longer possible to derive a Fokker-Planck equation. Figure 2 shows the final distribution $\mathcal{P}(p_{at})$ of atomic momentum deduced from a numerical integration of Bloch equations for parameters corresponding to our experimental conditions. As expected, one clearly sees two narrow peaks emerging above the background around $\pm\hbar k$. Note that the half-width of each peak is narrower than the one-photon recoil energy. We have checked that an increase of the interaction time Θ increases the height and decreases the width of these peaks. The value of Θ leading to the largest area under the peaks depends on the shape of the ini-

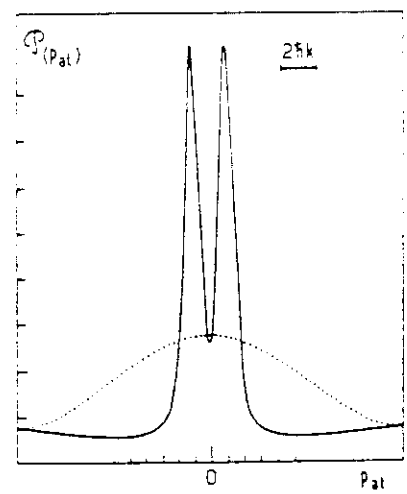

FIG. 2. Calculated transverse atomic momentum distribution resulting from cooling by velocity-selective coherent population trapping, for parameters close to our experimental situation (zero detuning, Rabi frequency $\omega_1 = 0.6\Gamma$, interaction time $\Theta = 350\Gamma^{-1}$). The initial distribution is represented by a dotted line.

tial distribution.

This cooling process has been demonstrated with the experimental setup shown in Fig. 3. A supersonic helium beam,[12] liquid-nitrogen cooled, is excited by counterpropagating electrons at 40 eV. The metastable He^* atoms in the 2^1S_0 state are optically quenched, and we obtain a beam of He^* in the 2^3S_1 state, with an intensity larger than 10^{12} atoms s^{-1} sr^{-1} and an average velocity of 1100 m s^{-1}. The He^* atoms interact on the 2^3S_1-2^3P_1 transition (1.083 μm) with a home-made single-mode ring version of a LNA laser[13] pumped by a 4-W Ar^+ laser. The laser frequency is locked to the atomic transition in an auxiliary discharge, by saturated-absorption techniques, and the laser linewidth is less than 1 MHz. After spatial filtering, the laser beam is expanded, passed through two quarter-wave plates (Fig. 3), and retroreflected, yielding two counterpropagating plane waves with opposite circular polarizations, with an almost uniform intensity in the 40-mm-diam interaction region (Rabi frequency $\omega_1 \simeq 0.6\Gamma$ with $\Gamma/2\pi \simeq 1.6$ MHz). There are stringent requirements for this experiment. First, the Zeeman, sublevels g_+ and g_- must remain degenerate in the whole interaction region. This condition is fulfilled by compensation of the magnetic field to less than 1 mG by Helmholtz coils and a Mumetal shield. Second, the relative phase between both laser beams must remain constant in the whole interaction region. This is achieved by our deriving both waves from the same laser beam and by using very high quality optical components for the second quarter-wave plate and for the retroreflecting mirror (wave-front distortion less than $\lambda/8$). Also, the exact overlap of the two beams is adjusted to 10^{-5} rad by autocollimation techniques. The transverse velocity distribution after the interaction zone is deduced from a transverse scan of an electron multiplier (sensitive to He^*) with a 100-μm entrance slit, placed downstream at 1.4 m from a first 100-μm slit just after the interaction region. The corresponding HWHM transverse velocity resolution is 4 cm s^{-1}.

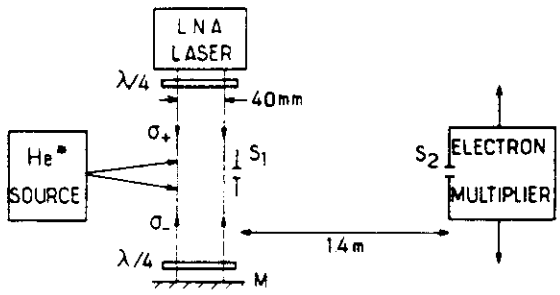

FIG. 3. Schematic experimental setup. The atomic source at 77 K produces a beam of metastable triple helium atoms (2^3S_1) at an average velocity of 1100 m/s. These atoms interact with two σ_+ and σ_- polarized counterpropagating waves at 1.08 μm. The transverse velocity distribution at the end of the interaction region is analyzed with two slits S_1 and S_2, 100 μm wide. S_2 is the entrance slit of a movable He^* detector.

Figure 4 shows the transverse velocity profiles with and without laser. The two peaks at about $\pm \hbar k/M$ (± 9.2 cm s^{-1}) clearly appear well above the initial distribution. A measurement of the standard half-width at $\exp(-\frac{1}{2})$ gives 6 cm/s, which corresponds to a temperature of about 2 μK. This experimental curve is in reasonable agreement with the theoretical prediction. Finer details concerning, for example, the variations of the efficiency of the cooling effect with the detuning still require further investigation.

We have performed supplementary tests to support the theoretical analysis given above. First, we replaced the σ_+ and σ_- circularly polarized beams by two orthogonally linearly polarized beams, and we checked that the final velocity distribution still presents two peaks at $\pm \hbar k/M$. On the contrary, for parallel linear polarizations where the nonabsorbing atomic superposition is not velocity selective, the two peaks at $\pm \hbar k/M$ disappear. Another test consists of our arranging the laser beams so that they do not exactly overlap at the end of the interaction region, the last acting laser beam being the σ_+ one. One expects atoms to be removed from the $|g_-, -\hbar k\rangle$ component of $|\psi_{NA}(0)\rangle$ and to be pumped after a few cycles (two on the average) into g_+ with a momentum spread around $+\hbar k$. Indeed, we have observed that the peak at $-\hbar k$ disappears while the peak at $+\hbar k$ increases and is broadened.

We have thus demonstrated that this velocity-selective optical pumping into a nonabsorbing state is a very efficient process to accumulate atoms in an extremely narrow velocity class. By increasing the coherent interaction time, still narrower velocity distributions could

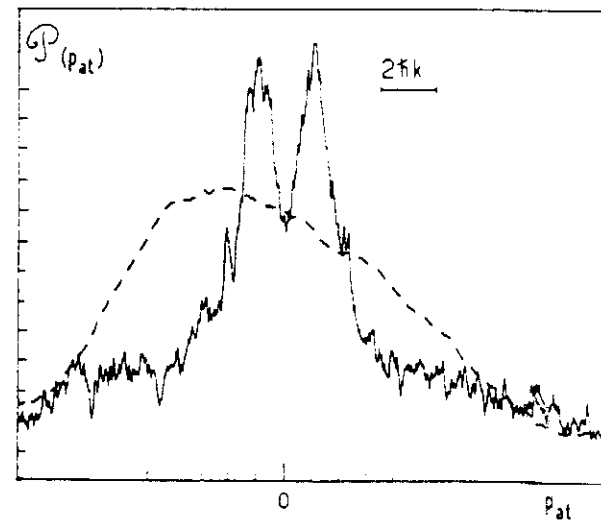

FIG. 4. Transverse atomic momentum profile at the end of the interaction region, with the laser on (solid line) and off (dashed line; this profile has been smoothed). The double-peak structure at about $\pm \hbar k$ and above the initial distribution is a clear signature of the cooling effect presented in this Letter.

be produced, allowing one to reach temperatures in the nanokelvin range. Several developments of this work can be considered: extensions to other level schemes; direct observation of the coherence between the two components of $|\psi_{NA}(0)\rangle$ propagating along different directions; generalization to three dimensions.

Finally, let us emphasize that this cooling mechanism is quite different from the previously demonstrated ones, since it is not due to a friction force but to diffusion into the cooled velocity class. Another important feature is that the cooled atoms no longer interact with the laser field which then causes no perturbation, either on external degrees of freedom (no diffusion) or on internal degrees of freedom (no light shifts). This particularity may be essential for future applications.

We warmly thank our colleagues Jean Dalibard and Christophe Salomon for very useful contributions to this work. This work is part of an operation supported by the stimulation program of European Economic Community. We have benefitted from crucial help from Helmut Haberland and Martin Karrais with the He^* atomic beam. Laboratoire de Spectroscopie Hertzienne de l'Ecole Normale Supérieure is Laboratoire No. 18 associé au Centre National de la Recherche Scientifique.

---

[a]Permanent address: Dipartimento di Fisica, Università di Pisa, I-56100 Pisa, Italy.

[1]D. J. Wineland and W. M. Itano, Phys. Rev. A 20, 1521 (1979); J. P. Gordon and A. Ashkin, Phys. Rev. A 21, 1606 (1980).

[2]H. Dehmelt, G. Janik, and W. Nagourney, Bull. Am. Phys. Soc. 30, 612 (1985); P. E. Toschek, Ann. Phys. (Paris) 10, 761 (1985).

[3]M. Lindberg and J. Javanainen, J. Opt. Soc. Am. B 3, 1008 (1986).

[4]P. D. Lett, R. N. Watts, C. I. Westbrook, W. D. Phillips, P. L. Gould, and H. J. Metcalf, Phys. Rev. Lett. 61, 169 (1988).

[5]See the contributions of J. Dalibard *et al.* and S. Chu, in Proceedings of the Eleventh International Conference on Atomic Physics, edited by S. Haroche, J. C. Gay, and G. Grynberg (World Scientific, Singapore, to be published).

[6]D. E. Pritchard, K. Helmerson, V. S. Bagnato, G. P. Lafyatis, and A. G. Martin, in *Laser Spectroscopy VIII*, edited by S. Svanberg and W. Persson (Springer-Verlag, Heidelberg, 1987), p. 68.

[7]First experimental observation in G. Alzetta, A. Gozzini, L. Moi, and G. Orriols, Nuovo Cimento 36B, 5 (1976); analyses in E. Arimondo and G. Orriols, Lett. Nuovo Cimento 17, 333 (1976); H. R. Gray, R. W. Whitley, and C. R. Stroud, Opt. Lett. 3, 218 (1978).

[8]V. G. Minogin and Yu. V. Rozhdestvenskii, Zh. Eksp. Teor. Fiz. 88, 1950 (1985) [Sov. Phys. JETP 61, 1156 (1985)]. The theoretical treatment of these authors is valid only for atomic momenta p larger than the photon momentum $\hbar k$ since their Fokker-Planck equation is based on an expansion in powers of $\hbar k/p$.

[9]Although we use here a classical description of the laser field, the matrix elements of $\exp(\pm ikz)$ appearing in V introduce the conservation laws for the total momentum.

[10]Semiclassical arguments can help one to understand the properties of $|\psi_{NA}(p)\rangle$. In the laser configuration of Fig. 1(a), the polarization of the total laser electric field E_L is linear and forms a helix along Oz with a pitch λ. For an atom in $|\psi_{NA}(p)\rangle$ the transition dipole moment d between $|\psi_{NA}, p\rangle$ and $|e_0, p'\rangle$ is also linearly polarized and forms a similar helix with the same pitch. The important point is that d is perpendicular to E_L for all z, so that the coupling is zero. Furthermore, the "laser helix" is at rest (since both lasers have the same frequency) whereas the "atomic helix" moves along Oz with a velocity p/M. Only for $p=0$ do both helices keep orthogonal polarizations for all times.

[11]Generalized optical Bloch equations have been discussed in detail by R. J. Cook, Phys. Rev. A 22, 1078–1098 (1980).

[12]H. Conrad, G. Ertl, J. Küppers, W. Sesselmann, and H. Haberland, Surf. Sci. 121, 161 (1982).

[13]L. D. Schearer, M. Leduc, D. Vivien, A. M. Lejus, and J. Thery, IEEE J. Quantum Electron. 22, 713 (1986).

Laser cooling below the one-photon recoil energy by velocity-selective coherent population trapping: theoretical analysis

A. Aspect, E. Arimondo,* R. Kaiser, N. Vansteenkiste, and C. Cohen-Tannoudji

Collège de France et Laboratoire de Spectroscopie Hertzienne de l'Ecole Normale Supérieure (Laboratoire Associé au Centre National de la Recherche Scientifique et à l'Université Paris VI), 24 Rue Lhomond, F 75231 Paris Cedex 05, France

Received April 3, 1989; accepted June 29, 1989

We present a theoretical analysis of a new one-dimensional laser-cooling scheme that was recently demonstrated on a beam of metastable ^{4}He atoms. Both internal and translational degrees of freedom are treated quantum mechanically. Unlike semiclassical approaches, such a treatment can be applied to situations in which the atomic coherence length is of the same order of or larger than the laser wavelength, which is the case for atoms cooled below the one-photon recoil energy. We introduce families of states that are closed with respect to absorption and stimulated emission, and we establish the generalized optical Bloch equations that are satisfied by the corresponding matrix elements. The existence of velocity-selective trapping states that are linear combinations of states with different internal and translational quantum numbers is demonstrated, and the mechanism of accumulation of atoms in these trapping states by fluorescence cycles is analyzed. From a numerical solution of the generalized optical Bloch equations, we study in detail how the final atomic-momentum distribution depends on the various physical parameters: interaction time, width of the initial distribution, laser detuning, laser power, and imbalance between the two counterpropagating waves. We show that the final temperature decreases when the interaction time increases, so that there is no fundamental limit to the lowest temperature that can be achieved by such a method. Finally, possible extensions of this method to two-dimensional cooling are presented.

1. INTRODUCTION

Laser cooling uses momentum exchange between photons and atoms to reduce the kinetic energy of atoms. Since each elementary momentum transfer is equal to the photon momentum $\hbar k$, the one-photon recoil energy $E_R = \hbar^2 k^2/2M$ (M is the atomic mass) represents an important landmark in the energy scale. Recent developments in laser cooling have permitted researchers to reach the regime where the equilibrium atomic kinetic energy becomes of the order of a few E_R (Refs. 1–3) or even smaller than E_R.[4] In this new regime, where the elementary momentum transfer can no longer be considered a small quantity, the analogy between atomic motion in laser light and Brownian motion breaks down, and the Fokker–Planck description of laser cooling is no longer valid. A new theoretical treatment is thus required.

The purpose of this paper is to present a quantitative analysis of laser cooling below the one-photon recoil energy by velocity-selective coherent population trapping. A one-dimensional laser cooling of this type was recently demonstrated on a beam of metastable ^{4}He atoms.[4] Here we present equations of motion that permit a quantitative interpretation of such a cooling scheme, and we discuss their physical content as well as their solutions. The theoretical approach followed here can be also useful for the analysis of other situations in which temperatures of the order of the one-photon recoil energy are approached. For example, similar equations can be found in the analysis of laser-cooling schemes below the Doppler limit based on gradients of laser polarization[5] or in the investigation of the lowest temperature that can be reached by cooling with ultranarrow atomic transitions for which $\hbar\Gamma \lesssim E_R$, where Γ is the natural width of the line.[6]

To describe atomic motion in laser light, one usually starts from equations of motion that describe the coupled evolution of the internal and external (translational) atomic degrees of freedom as a result of resonant exchanges of energy and momentum between photons and atoms. Because of the discrete character of the photon momentum $\hbar k$, these equations are finite-difference equations. They are usually transformed into coupled partial differential equations through an expansion of the density-matrix elements in powers of $\hbar k/\Delta p$, where Δp is the width of the atomic-momentum distribution. For sufficiently slow atoms, one also makes an expansion in powers of $k\Delta p/M\Gamma$ (the ratio between the Doppler shift and the natural width). Finally, after an adiabatic elimination of the fast internal variables, one gets, for the atomic Wigner function, a Fokker–Planck equation that allows one to consider atomic motion in laser light as a Brownian motion and that provides theoretical expressions for the friction coefficient γ and the diffusion coefficient D and consequently for the equilibrium temperature T ($k_B T \sim D/M\gamma$).[7]

The previous theoretical scheme is valid only if the expansion parameter $\hbar k/\Delta p$ is very small, i.e., if the atomic coherence length $\hbar/\Delta p$ is small compared with the laser wavelength $\lambda = 2\pi/k$. When the energy $k_B T = p^2/2M$ becomes of the order of or smaller than the recoil energy $E_R = \hbar^2 k^2/2M$, we reach a new regime where the coherence length $\hbar/\Delta p$ becomes longer than the laser wavelength λ. It is then no longer possible to consider the atomic wave packet to be well localized in the laser wave and to describe its motion by a

0740-3224/89/112112-13$02.00

Fokker–Planck equation. We must return to the full quantum coupled equations of motion. This is precisely what we do in this paper.

The paper is organized as follows. In Section 2 we give the level scheme and the laser configuration that are used in the new laser-cooling method, whose principle is briefly explained. We show in Section 3 that, for two counterpropagating σ_+ and σ_- circularly polarized laser waves, the absence of redistribution of photons between the two waves allows us to introduce a finite number of states, labeled by external and internal quantum numbers, and that are coupled by absorption and stimulated-emission processes. These closed families of states are the basic ingredient of this paper. In Section 3 we give the equations of motion of the density-matrix elements within such a family as a result of absorption and stimulated emission, and in this way we interpret the principle of velocity-dependent coherent population trapping. Spontaneous emission plays an important role in redistributing atoms among the different families. The corresponding equations are established and discussed in Section 4. It is then possible to write in Section 5 the full equations of motion as well as of the initial state and the detection signal. Numerical solutions of these equations are presented in Section 6, and the influence of the various physical parameters is discussed in detail. Finally, a possible extension of this new cooling scheme is considered in Section 7.

2. SIMPLE PRESENTATION OF THE NEW LASER-COOLING SCHEME

The new scheme uses a three-level Λ configuration in which two degenerate ground sublevels $g_\pm$ are coupled to an excited level e_0 by two counterpropagating σ_+ and σ_- polarized laser beams with the same frequency ω_L [Fig. 1(a)]. In the experiment described in Ref. 4, $g_\pm$ are the two Zeeman sublevels $m = \pm 1$ of the 2^3S_1 state of ^{4}He, whereas e_0 is the $m = 0$ Zeeman sublevel of 2^3P_1 [the Clebsch–Gordan coefficient between 2^3S_1 ($m = 0$) and 2^3P_1 ($m = 0$) vanishes, permitting us to ignore the 2^3S_1 ($m = 0$) state in what follows].

First consider an atom at rest. For such an atom the two apparent laser frequencies are equal, and resonant processes involving one interaction with each beam can take place between g_+ and g_-. We can then show that there is a coherent superposition of g_+ and g_- that is not coupled to e_0 by the laser excitation. Such a situation occurs when the two amplitudes for absorbing a σ_+ or a σ_- photon interfere destructively. For example, if the two excitation amplitudes $g_+ \rightarrow e_0$ and $g_- \rightarrow e_0$ are equal, the nonabsorbing coherent superposition of g_+ and g_- is just $(|g_+\rangle - |g_-\rangle)/\sqrt{2}$. An atom put in such a superposition of states remains trapped there indefinitely since it can no longer absorb light. Such a mechanism of coherent population trapping owing to destructive interference between two excitation amplitudes is actually quite general and can give rise to narrow resonances. It was discovered in 1976,[8] and several theoretical treatments based on optical Bloch equations[9] or on the dressed-atom approach[10,11] have been given.

Coming back to the scheme of Fig. 1(a), we suppose now that the atom is moving along Oz. The Raman resonance condition is no longer fulfilled as a consequence of opposite Doppler shifts on the two counterpropagating laser beams.

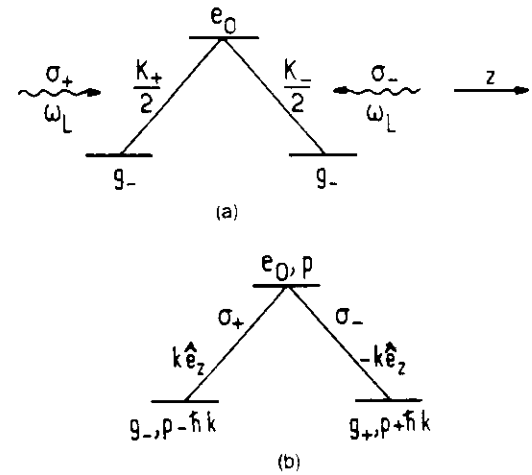

Fig. 1. Three-level Λ configuration. (a) Two degenerate ground sublevels $g_\pm$ are coupled to an excited level e_0 by two counterpropagating σ_+ and σ_- circularly polarized laser beams with the same frequency ω_L; the corresponding coupling matrix elements are $K_+/2$ and $K_-/2$ in frequency units. (b) Closed family of states coupled by interaction with the two lasers. Each state is characterized by its internal quantum number and its linear momentum along Oz.

It follows that the two excitation amplitudes $g_+ \rightarrow e_0$ and $g_- \rightarrow e_0$ can no longer interfere destructively. This simple argument explains how the phenomenon of coherent population trapping can be velocity selective for appropriate laser configurations.[12] The new cooling scheme discussed in this paper consists of accumulating atoms in the zero-velocity nonabsorbing state where they remain trapped. To populate this state, we take advantage of the momentum redistribution due to spontaneous emission, which allows certain atoms to be pumped optically from the absorbing velocity classes into the nonabsorbing state. Since the recoil of the last spontaneous-emission photon is part of the cooling mechanism, the one-photon recoil energy is not a limit, and the final temperature is limited only by the coherent interaction time.[13] Note also that, unlike other cooling schemes, our mechanism, based on a Raman resonance condition, does not depend on the sign of the laser detuning.

However, the previous analysis is too crude. Since the two laser waves propagate in opposite directions, the phases of the two electric fields, and consequently the phases of the two excitation amplitudes $g_- \rightarrow e_0$ and $g_+ \rightarrow e_0$, vary as $\exp(ikz)$ and $\exp(-ikz)$, respectively. It follows that, for an atom at z, the nonabsorbing superposition of states must be written as

$$\frac{1}{\sqrt{2}}\left[\exp(ikz)|g_+\rangle - \exp(-ikz)|g_-\rangle\right] \tag{2.1}$$

and depends on z. On the other hand, when the atoms get very cold ($\Delta p \ll \hbar k$), their coherence length becomes large compared with λ, and it is no longer possible to restrict the discussion to atoms localized at a given z. This shows that the nonabsorbing state must actually be described by an extended spinor or vector wave function of the type of expression (2.1), which exhibits strong correlations between internal and external degrees of freedom. A more rigorous analysis thus requires the introduction of a basis of states involving both internal and translational quantum numbers

and that we expand the atomic state vector (or density matrix) on such a basis. That is what we do in Section 3.

3. CLOSED FAMILIES OF STATES COUPLED BY ABSORPTION AND STIMULATED EMISSION

A. Physical Idea and Notation

Let us introduce the state $|e_0, p\rangle$, which represents an atom in the excited state e_0 with a linear momentum p along Oz ($p_{at}^z = p$, where $\mathbf{p}_{at}$ is the atomic momentum). Because of angular-momentum conservation, the interaction with the σ_+ circularly polarized wave (stimulated emission or absorption) can couple together only e_0 and g_-. On the other hand, because of linear-momentum conservation, such an interaction with a wave propagating toward $+Oz$ involves the exchange of a photon of momentum $+\hbar k$ and thus can couple only $|e_0, p\rangle$ and $|g_-, p - \hbar k\rangle$. Similarly, the interaction of the atom with the σ_- circularly polarized wave propagating toward $-Oz$ can couple only $|e_0, p\rangle$ and $|g_+, p + \hbar k\rangle$ [Fig. 1(b)].

We are thus led to introduce a family of three states coupled by absorption or stimulated emission:

$$\mathcal{F}(p) = \{|e_0, p\rangle, |g_-, p - \hbar k\rangle, |g_+, p + \hbar k\rangle\}. \tag{3.1}$$

As long as spontaneous emission is not taken into account, this is a closed family of coupled states.

When considering the evolution of the density-matrix elements due to absorption and stimulated emission, strong selection rules appear. For instance, $\langle e_0, p'|\sigma|e_0, p''\rangle$ is coupled only to $\langle g_\pm, p' \pm \hbar k|k\sigma|e_0, p''\rangle$ and $\langle e_0, p'|\sigma|g_\pm, p'' \pm \hbar k\rangle$. A further simplification happens because all the interesting quantities that we need to calculate (see Section 5 below) are terms such as $\langle e_0, p|\sigma|e_0, p\rangle$, $\langle g_+, p|\sigma|g_+, p\rangle$, $\langle g_-, p|\sigma|g_-, p\rangle$, and $\langle g_-, p - \hbar k|\sigma|g_+, p + \hbar k\rangle$. These terms are coupled only to terms internal in the family. For example, $\langle e_0, p|\sigma|e_0, p\rangle$ is coupled only to $\langle g_\pm, p \pm \hbar k|\sigma|e_0, p\rangle$ and $\langle e_0, p|\sigma|g_\pm, p \pm \hbar k\rangle$. In summary, the evolution equations relevant to the problem under discussion will involve only density-matrix elements defined inside a family $\mathcal{F}(p)$. For such elements, we use the simplified notation,

$$\sigma_{ee}(p) = \langle e_0, p|\sigma|e_0, p\rangle, \tag{3.2a}$$

$$\sigma_{\pm\pm}(p) = \langle g_\pm, p \pm \hbar k|\sigma|g_\pm, p \pm \hbar k\rangle, \tag{3.2b}$$

$$\sigma_{e\pm}(p) = \langle e_0, p|\sigma|g_\pm, p \pm \hbar k\rangle, \tag{3.2c}$$

$$\sigma_{\pm e}(p) = [\sigma_{e\pm}(p)]^*. \tag{3.2d}$$

We show below that, although spontaneous emission couples different families, it involves only coupling with terms of the type defined in Eqs. (3.2). For instance, $\sigma_{ee}(p)$ can decay only to terms such as $\sigma_{++}(p')$ and $\sigma_{--}(p')$. The elements defined in Eqs. (3.2) are thus the only ones that we have to consider.

Remarks

(i) The notion of closed families of states is central in the analysis presented in this paper. It must be emphasized that closed families exist only for specific level schemes and laser wave configurations.[14] In the standard situation when a two-level atom interacts with two counterpropagating linearly polarized waves, $|e, p\rangle$ is coupled to $|g, p - \hbar k\rangle$ and $|g, p + \hbar k\rangle$, which are themselves coupled to $|e, p\rangle$, $|e, p - 2\hbar k\rangle$, and $|e, p + 2\hbar k\rangle$, etc. In such a situation, each family has an infinite number of coupled states. Families of this type have been already considered (see, for example, Ref. 15).

(ii) The quantity p appearing in Eq. (3.1) or Eqs. (3.2) is just a label used to index a family. We will see below that it can be interpreted as the total linear momentum (modulo $\hbar k$) of the atoms + laser field system, which is an invariant quantity of the family.

B. Evolution Equations

We now write the equations describing the evolution of the atom interacting with the laser field, taken as a classical field. Here we do not yet take spontaneous emission into account, and we consider only absorption and stimulated-emission processes. The corresponding Hamiltonian is the sum of two parts:

$$H = H_A + V, \tag{3.3}$$

where H_A is the Hamiltonian of the free atom and V is the laser–atom coupling. H_A is the sum of the kinetic and internal energies:

$$H_A = \frac{\mathbf{P}^2}{2M} + \hbar\omega_0|e_0\rangle\langle e_0|. \tag{3.4}$$

In order to simplify the equations, we consider here the case when the two ground states $|g_+\rangle$ and $|g_-\rangle$ have the same internal energy, taken equal to zero. The formalism developed in this paper could easily be generalized to the case when the energies E_{g_+} and E_{g_-} are different, and the physics would be the same provided that the two laser frequencies differ by $(E_{g_+} - E_{g_-})/\hbar$.

The coupling Hamiltonian is

$$V = -\mathbf{D}\cdot\mathbf{E}(z, t), \tag{3.5}$$

where $\mathbf{D}$ is the electric-dipole-moment operator and $\mathbf{E}(z, t)$ is the classical electric field:

$$\mathbf{E}(z, t) = \tfrac{1}{2}\{\epsilon_+ E_+ \exp[i(kz - \omega_L t) + \text{c.c.}]\} + \tfrac{1}{2}\{\epsilon_- E_- \exp[i(-kz - \omega_L t) + \text{c.c.}]\}, \tag{3.6}$$

(where c.c is the complex conjugate). The first term corresponds to a σ_+ circularly polarized wave propagating toward $z > 0$, while the second one corresponds to a σ_- circularly polarized wave propagating toward $z < 0$ [$\epsilon_\pm = \mp(\mathbf{e}_x \pm i\mathbf{e}_y)/\sqrt{2}$].

The coupling of the atom with each of these waves is characterized by the Rabi frequencies K_+ and K_-:

$$K_\pm = -\frac{d_\pm E_\pm}{\hbar}, \quad d_\pm = \langle e_0|\epsilon_\pm\cdot\mathbf{D}|g_\pm\rangle. \tag{3.7a}$$

Note the selection rules

$$\langle e_0|\epsilon_+\cdot\mathbf{D}|g_+\rangle = \langle e_0|\epsilon_-\cdot\mathbf{D}|g_-\rangle = 0, \tag{3.7b}$$

which can be interpreted in terms of conservation of angular momentum. With the rotating wave approximation, V can be written as

$$V = \left[\frac{\hbar K_+}{2}|e_0\rangle\langle g_-|\exp(ikz) + \frac{\hbar K_-}{2}|e_0\rangle\langle g_+| \times \exp(-ikz)\right]\exp(-i\omega_L t) + \text{H.c.} \quad (3.8)$$

(where H.c. is the Hermitian conjugate).

Note that in Eq. (3.8) z is an operator acting on the external degrees of freedom of the atom. Using the relation

$$\exp(\pm ikz) = \sum_p |p\rangle\langle p \mp \hbar k|,$$

we finally get

$$V = \sum_p \left[\frac{\hbar K_+}{2}|e_0, p\rangle\langle g_-, p - \hbar k| + \frac{\hbar K_-}{2}|e_0, p\rangle\langle g_+, p + \hbar k|\right] \times \exp(-i\omega_L t) + \text{H.c.} \quad (3.9)$$

It clearly appears from Eq. (3.9) that $|e, p\rangle$ is coupled only to $|g_-, p - \hbar k\rangle$ and $|g_+, p + \hbar k\rangle$. As was already emphasized in Subsection 3.A, the atom–laser interaction can induce transitions only inside the closed family $\mathcal{F}(p)$. The evolution of such a family is thus described by a closed set of equations among the nine density matrix elements characterizing the family at time t [Eq. (3.2)].

In order to eliminate time-dependent coefficients, it is useful to make the usual transformation

$$\begin{aligned}\tilde\sigma_{e\pm}(p) &= \sigma_{e\pm}\exp(i\omega_L t),\\ \tilde\sigma_{+-}(p) &= \sigma_{+-}(p),\\ \tilde\sigma_{ii}(p) &= \sigma_{ii}(p) \qquad (i = +, -, e).\end{aligned} \quad (3.10)$$

The evolution equations are then

$$\left[\frac{d}{dt}\tilde\sigma_{--}(p)\right]_{\text{Ham}} = -i\frac{K_+^*}{2}\tilde\sigma_{e-}(p) + \text{c.c.},$$

$$\left[\frac{d}{dt}\tilde\sigma_{++}(p)\right]_{\text{Ham}} = -i\frac{K_-^*}{2}\tilde\sigma_{e+}(p) + \text{c.c},$$

$$\left[\frac{d}{dt}\tilde\sigma_{ee}(p)\right]_{\text{Ham}} = i\frac{K_+^*}{2}\tilde\sigma_{e-}(p) + i\frac{K_-^*}{2}\tilde\sigma_{e+}(p) + \text{c.c},$$

$$\left[\frac{d}{dt}\tilde\sigma_{e+}(p)\right]_{\text{Ham}} = i\left(\delta_L + k\frac{p}{M} + \omega_R\right)\tilde\sigma_{e+}(p) - i\frac{K_-}{2}[\tilde\sigma_{++}(p) - \tilde\sigma_{ee}(p)] - i\frac{K_+}{2}\tilde\sigma_{-+}(p),$$

$$\left[\frac{d}{dt}\sigma_{e-}(p)\right]_{\text{Ham}} = i\left(\delta_L - k\frac{p}{M} + \omega_R\right)\tilde\sigma_{e-}(p) - i\frac{K_+}{2}[\tilde\sigma_{--}(p) - \tilde\sigma_{ee}(p)] - i\frac{K_-}{2}\tilde\sigma_{-+}{}^*(p),$$

$$\left[\frac{d}{dt}\tilde\sigma_{-+}(p)\right]_{\text{Ham}} = -i\frac{K_+^*}{2}\tilde\sigma_{e+}(p) + i\frac{K_-}{2}\tilde\sigma_{e-}{}^*(p) + 2ik\frac{p}{M}\tilde\sigma_{-+}(p), \quad (3.11)$$

and three complex-conjugated equations.

These equations generalize the usual optical Bloch equations by including external quantum numbers.[16] We have called $\omega_R = \hbar k^2/2M$ the recoil frequency shift and $\delta_L = \omega_L - \omega_0$ is the laser detuning. Note that kp/M is the Doppler shift associated with the velocity p/M.

C. Velocity-Selective Coherent Population Trapping

The evolution equations [Eqs. 3.11)] allow us to understand how coherent population trapping is velocity selective in the configuration considered here. Let us consider the following two orthogonal linear combinations of $|g_+, p + \hbar k\rangle$ and $|g_-, p - \hbar k\rangle$:

$$|\psi_{\text{NC}}(p)\rangle = \frac{K_-}{(|K_+|^2 + |K_-|^2)^{1/2}}|g_-, p - \hbar k\rangle - \frac{K_+}{(|K_+|^2 + |K_-|^2)^{1/2}}|g_+, p + \hbar k\rangle, \quad (3.12a)$$

$$|\psi_{\text{C}}(p)\rangle = \frac{K_+^*}{(|K_+|^2 + |K_-|^2)^{1/2}}|g_-, p - \hbar k\rangle + \frac{K_-^*}{(|K_+|^2 + |K_-|^2)^{1/2}}|g_+, p + \hbar k\rangle. \quad (3.12b)$$

The reason for introducing $|\psi_{\text{NC}}(p)\rangle$ is that, according to Eq. (3.9), the transition matrix element between $|\psi_{\text{NC}}(p)\rangle$ and $|e_0, p\rangle$ vanishes:

$$\langle e, p|V|\psi_{\text{NC}}(p)\rangle = 0. \quad (3.13a)$$

Consequently, an atom in the noncoupled state $|\psi_{\text{NC}}(p)\rangle$ cannot absorb a laser photon, and it cannot be excited to $|e_0, p\rangle$. A similar calculation gives

$$\langle e_0, p|V|\psi_{\text{C}}(p)\rangle = \frac{\hbar}{2}(|K_+|^2 + |K_-|^2)^{1/2}\exp(-i\omega_L t) \quad (3.13b)$$

and shows that $|\psi_{\text{C}}(p)\rangle$ is coupled to the excited state.

We now suppose that an atom has been prepared at a certain time in $|\psi_{\text{NC}}(p)\rangle$, and we study its subsequent evolution. Equations (3.11) and (3.12) lead to the following equation of motion for $\langle\psi_{\text{NC}}(p)|\sigma|\psi_{\text{NC}}(p)\rangle$:

$$\frac{d}{dt}\langle\psi_{\text{NC}}(p)|\sigma|\psi_{\text{NC}}(p)\rangle = -ik\frac{p}{M}\frac{2K_+K_-}{|K_+|^2 + |K_-|^2} \times \langle\psi_{\text{NC}}(p)|\sigma|\psi_{\text{C}}(p)\rangle + \text{c.c.} \quad (3.14)$$

Suppose first that $p = 0$. The right-hand side of Eq. (3.14) then vanishes. This means that an atom prepared in $|\psi_{\text{NC}}(0)\rangle$ cannot leave this state either by free evolution (effect of the free Hamiltonian H_A) or by absorption of a laser photon (effect of the laser–atom coupling V). Although we have not yet taken spontaneous emission into account, it is clear also that the atom cannot leave $|\psi_{\text{NC}}(0)\rangle$ by spontaneous emission since this state is, according to Eq. (3.12a), a linear combination of two ground states $|g_+\rangle$ and $|g_-\rangle$, which are both radiatively stable. To conclude, the state $|\psi_{\text{NC}}(0)\rangle$ is a perfect trap since an atom prepared in this state remains there indefinitely.

On the other hand, if $p \neq 0$, Eq. (3.14) shows that there is a coupling proportional to kp/M (coming from the free Hamil-

tonian H_A) between $|\psi_{NC}(p)\rangle$ and $|\psi_C(p)\rangle$. This means that an atom initially in $|\psi_{NC}(p)\rangle$ can be transferred by H_A to $|\psi_C(p)\rangle$ and from there to $|e_0, p\rangle$ by V [see Eq. (3.13b)]. The state $|\psi_C(p)\rangle$ cannot therefore be considered a perfect trap when $p \neq 0$, since excitation by the laser can take place after an intermediate transition to $|\psi_C(p)\rangle$. Interpreting p/M as the atomic velocity in the excited state of the family $\mathcal{F}(p)$, we thus see that coherent population trapping in $|\psi_{NC}(p)\rangle$ is velocity selective, since it happens only for $p = 0$.

The motional coupling between $|\psi_{NC}(p)\rangle$ and $|\psi_C(p)\rangle$ appearing in Eq. (3.14) can also be interpreted by noticing that when $p \neq 0$ the kinetic energies of $|g_-, p - \hbar k\rangle$ and $|g_+, p + \hbar k\rangle$ differ by $2\hbar kp/M$. It appears clearly from Eqs. (3.12) that, in this case ($p \neq 0$), $|\psi_{NC}(p)\rangle$ and $|\psi_C(p)\rangle$ are not stationary with respect to H_A; consequently H_A induces an oscillation between these two states. It is easy to show that the Rabi frequency of this oscillation is just $2kp/M$, which is also the beat note between the two Doppler-shifted laser frequencies. The visibility of this oscillation is maximum (equal to 1) when the intensities are equal ($|K_+| = |K_-|$).

Remarks

(i) The various couplings between $|\psi_C(p)\rangle$, $|\psi_{NC}(p)\rangle$, and $|e_0, p\rangle$ due to H_A and V are represented in Fig. 2. $|\psi_C(p)\rangle$ and $|\psi_{NC}(p)\rangle$ are coupled by the motional term kp/M; $|\psi_C(p)\rangle$ and $|e_0, p\rangle$ are coupled by the atom–laser interaction $K/\sqrt{2}$ (here we take $K_+ = K_- = K$). Although we have not yet introduced spontaneous emission, we know that $|e_0, p\rangle$ has a natural width Γ. It follows that for a resonant excitation ($\delta_L = 0$), and in the weak-intensity limit ($K \ll \Gamma$), the Rabi coupling $K/\sqrt{2}$ between $|\psi_C(p)\rangle$ and the broad state $|e_0, p\rangle$ gives to the state $|\psi_C(p)\rangle$ a finite width

$$\Gamma' = 2K^2/\Gamma. \tag{3.15}$$

The same argument shows that the motional coupling kp/M between $|\psi_{NC}(p)\rangle$ and the state $|\psi_C(p)\rangle$ with a width Γ' gives to $|\psi_{NC}(p)\rangle$ a finite width Γ'', which, in the limit $kp/M \ll \Gamma'$, is equal to

$$\Gamma'' = \frac{2(kp/M)^2\Gamma}{K^2}. \tag{3.16}$$

Γ'' is the probability per unit time of an atom's leaving the state $|\psi_{NC}(p)\rangle$. The smaller p, the longer the time an atom can be trapped in $|\psi_{NC}(p)\rangle$. Consider an interaction time Θ. Only atoms with p such that $\Gamma''\Theta < 1$, i.e., such that

$$\left(\frac{kp}{M}\right)^2 < \frac{K^2}{2\Theta\Gamma}, \tag{3.17}$$

can remain trapped in the noncoupled state during Θ.

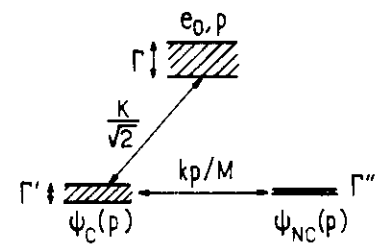

Fig. 2. Couplings and level widths for the three states $|e_0, p\rangle$, $|\psi_C(p)\rangle$, and $|\psi_{NC}(p)\rangle$ of the family $\mathcal{F}(p)$. $|\psi_C(p)\rangle$ is coupled to $|e_0, p\rangle$ by the laser (coupling matrix element $K/\sqrt{2}$). $|\psi_{NC}(p)\rangle$ is coupled to $|\psi_C(p)\rangle$ by the motion (coupling matrix element kp/M). As a result of these couplings, $|\psi_C(p)\rangle$ and $|\psi_{NC}(p)\rangle$ acquire finite widths Γ' and Γ'', respectively (departure rates). Γ is the natural width of $|e_0, p\rangle$.

(ii) One can give a classical picture of velocity-selective coherent population trapping for the situation considered here. The electric field [Eq. (3.6)] is linearly polarized at every point, with the direction of polarization changing with z as a helix of pitch λ. On the other hand, for a state $|\psi_{NC}(p)\rangle$ the transition electric-dipole moment between the state $|\psi_{NC}(p)\rangle$ and the excited state $|e_0, p\rangle$ also makes a helix with the same pitch λ, orthogonal everywhere to the electric field, so that the coupling is zero. For a state $|\psi_C(p)\rangle$ the transition-dipole moment makes a similar helix shifted by $\lambda/4$, and it is parallel everywhere to the electric field, so that the coupling is maximum. Suppose now that an atom is in the state $|\psi_{NC}(p)\rangle$ at a given time; the transition-dipole-moment helix will move along Oz with a velocity p/M, so that the probability of the atom's being in $|\psi_C(p)\rangle$ (i.e., to be excited to $|e_0, p\rangle$) will be modulated at the frequency $2kp/M$. If $p = 0$, the transition electric-dipole-moment helix does not move. It remains orthogonal to the electric-field helix indefinitely, and the atom cannot be excited to $|e_0, p\rangle$: it is thus trapped in $|\psi_{NC}(0)\rangle$.

4. SPONTANEOUS EMISSION

A. Redistribution among Families

In Section 3 we showed that an atom prepared in $|\psi_{NC}(0)\rangle$ cannot leave this state by any process. We now have to explain how atoms can be prepared in such a state. In this respect, spontaneous emission plays a basic role since it allows atoms to jump from one family to another one. In particular, atoms can be optically pumped from a family $\mathcal{F}(p \neq 0)$ into the family $\mathcal{F}(p = 0)$ where they may get trapped in the $|\psi_{NC}(0)\rangle$ state.

Consider an atom in the excited state $|e_0, p\rangle$ of the family $\mathcal{F}(p)$. It can emit by spontaneous emission a fluorescence photon in any direction. Suppose that the fluorescence photon has a linear momentum u along Oz (u can take any value between $-\hbar k$ and $+\hbar k$). Because of the law of momentum conservation, the atomic momentum changes by $-u$, so that, in such a process, the atom makes a transition from $|e_0, p\rangle$ to $|g_+, p - u\rangle$ [Fig. 3(a)] or to $|g_-, p - u\rangle$ [Fig. 3(b)] or to a linear superposition of these two states. Note that the two states $|g_\pm, p - u\rangle$ do not in general belong to the same family as $|e_0, p\rangle$: $|g_+, p - u\rangle$ belongs to $\mathcal{F}(p - u - \hbar k)$ and $|g_-, p - u\rangle$ to $\mathcal{F}(p - u + \hbar k)$ (see Fig. 3). Spontaneous emission can thus redistribute atoms from the family $\mathcal{F}(p)$ to any family $\mathcal{F}(p')$, with

$$p - 2\hbar k \leqslant p' \leqslant p + 2\hbar k. \tag{4.1}$$

This diffusion in the family space provides the mechanism for accumulating atoms in the family $\mathcal{F}(p = 0)$.

B. Corresponding Terms in the Master Equation

The first effect of spontaneous emission is the usual damping of populations and coherences involving the excited state[17]

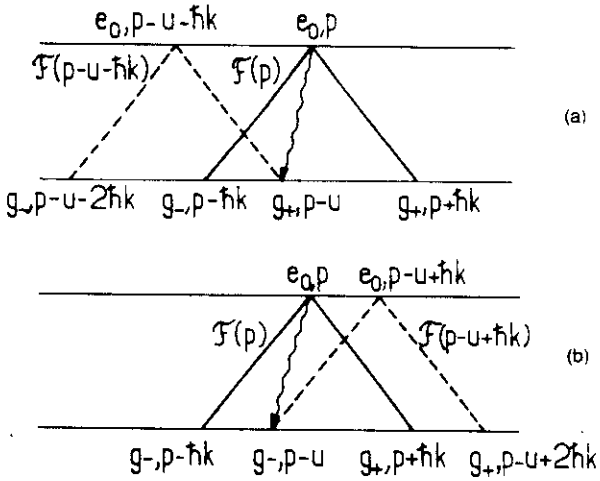

Fig. 3. Redistribution among families by spontaneous emission. Spontaneous emission of a photon with linear momentum u along Oz (wavy lines) can bring an atom from the family $\mathcal{F}(p)$ (solid lines) to the family $\mathcal{F}(p-u-\hbar k)$ [dashed lines in (a)] or to the family $\mathcal{F}(p-u+\hbar k)$ [dashed lines in (b)]. Each state is represented by a point with an abscissa equal to its atomic momentum along Oz and by its internal quantum number e_0 (upper horizontal line) or $g_\pm$ (lower horizontal line). The label of a family is the atomic momentum of its excited state.

$$\left[\frac{d}{dt}\sigma_{ee}(p)\right]_{sp} = -\Gamma\sigma_{ee}(p), \tag{4.2a}$$

$$\left[\frac{d}{dt}\sigma_{e+}(p)\right]_{sp} = -\frac{\Gamma}{2}\sigma_{e+}(p), \tag{4.2b}$$

$$\left[\frac{d}{dt}\sigma_{e-}(p)\right]_{sp} = -\frac{\Gamma}{2}\sigma_{e-}(p). \tag{4.2c}$$

The corresponding feeding terms in the ground state must take into account the redistribution among families introduced above. Consider, for example, $[d\sigma_{++}(p)/dt)_{sp}$, which gives the rate at which $|g_+, p+\hbar k\rangle$ can be populated by spontaneous emission. Such a state is populated from $|e_0, p+\hbar k+u\rangle$ [see Fig. 3(a)] with a rate $\Gamma_+ H(u)$, where $H(u)$ is the normalized probability

$$\int_{-\hbar k}^{+\hbar k} du H(u) = 1$$

that the emitted photon has a momentum u along Oz and Γ_+ is the deexcitation rate from the excited state e_0 to the state g_+; the oscillator strength of the transition $e_0 \rightarrow g_+$ having been taken into account:

$$\Gamma_+ = \Gamma/2.$$

Summing over u, one gets[17]

$$\left[\frac{d}{dt}\sigma_{++}(p)\right]_{sp} = \frac{\Gamma}{2}\int_{-\hbar k}^{+\hbar k} du H(u)\sigma_{ee}(p+\hbar k+u). \tag{4.3a}$$

A similar argument [see Fig. 3(b)] gives

$$\left[\frac{d}{dt}\sigma_{--}(p)\right]_{sp} = \frac{\Gamma}{2}\int_{-\hbar k}^{+\hbar k} du H(u)\sigma_{ee}(p+u-\hbar k). \tag{4.3b}$$

The kernel $H(u)$ depends on the radiation pattern for the $|e_0\rangle \rightarrow |g_\pm\rangle$ transitions.[18] For instance, in the $|J=1, m=0\rangle \rightarrow |J=1, m=\pm 1\rangle$ transition considered in Ref. 4,

$$H(U) = \frac{3}{8}\frac{1}{\hbar k}\left(1+\frac{u^2}{\hbar^2 k^2}\right). \tag{4.3c}$$

The possibility of feeding the coherences of the ground state $\sigma_{+-}(p)$ must also be considered. In fact, we are dealing here with Zeeman ground sublevels, and it is well known that such coherences can be fed only by corresponding coherences in the excited state. But here there is only one populated excited state, so we have no feeding term for these ground Zeeman coherences. More precisely, spontaneous emission of a photon $\hbar\mathbf{k}$ in a well-defined direction (and with a well-defined polarization) from the excited state $|e_0, \mathbf{p}\rangle$ will give rise to a well-defined coherence between $|g_+, \mathbf{p}-\hbar\mathbf{k}\rangle$ and $|g_-, \mathbf{p}-\hbar\mathbf{k}\rangle$. But, if we average over the azimuthal angle ϕ of $\mathbf{k}$, keeping the angle θ between Oz and $\mathbf{k}$ constant, and if we trace over the components of the atomic momentum perpendicular to Oz (which are not observed), we find that the coherence between $|g_+, p-u\rangle$ and $|g_-, p-u\rangle$ (where $p = p_z$ and $u = \hbar k\cos\theta$) vanishes. This is a consequence of the invariance of spontaneous emission in a rotation around Oz.

We must also discuss the question of external coherences, i.e., terms such as

$$\langle g_-, p'|\sigma|g_-, p''\rangle.$$

We can show that because of translational invariance for spontaneous emission in free space, such a term could be fed only by a corresponding coherence in the excited state, i.e., by a term

$$\langle e, p'-u|\sigma|e, p''-u\rangle.$$

In the problem considered here, we start from an initial distribution of atoms in the ground states $|g_-, p'\rangle$ and $|g_+, p''\rangle$, without any coherence between such terms. The coupling [Eq. (3.9)] cannot create external coherences in the excited state from such an initial state, and we can thus conclude that spontaneous emission will not feed external coherences in the ground state.

We have thus justified the statement of Subsection 3.A according to which the only density-matrix elements relevant to our problem are the elements defined in Eqs. (3.2), i.e., density-matrix elements defined inside a family $\mathcal{F}(p)$. We can also conclude that Eqs. (4.2) and (4.3) describe correctly the effect of spontaneous emission for the problem discussed in this paper.

C. Mechanism for Accumulating Atoms in the Trapping State

As is shown by Eqs. (4.3a) and (4.3b), spontaneous emission provides the mechanism for accumulating atoms in the trapping state: indeed, an atom in the excited state $|e_0, p\rangle$ with $0 \leq p \leq 2\hbar k$ can decay by spontaneous emission into $|g_+, +\hbar k\rangle$, which increases $\sigma_{++}(p=0)$ [see Fig. 3(a)]. Similarly, $|g_-, -\hbar k\rangle$ [corresponding to $\sigma_{--}(p=0)$] may be populated from any excited state $|e_0, p\rangle$ with $-2\hbar k \leq p \leq 0$.

Note, however, that although each of these ground states belongs to the $\mathcal{F}(p=0)$ family, an atom in $|g_+, +\hbar k\rangle$ or in $|g_-, -\hbar k\rangle$ is not yet in the trapping state $|\psi_{NC}(0)\rangle$. This requires a further step, namely, filtering in the state space. Take, for

instance, an atom in $|g_-, -\hbar k\rangle$. It can be considered as being in a linear superposition of $|\psi_{NC}(0)\rangle$ and $|\psi_C(0)\rangle$:

$$|g_-, -\hbar k\rangle = \frac{1}{\sqrt{2}} [|\psi_{NC}(0)\rangle + |\psi_C(0)\rangle] \tag{4.4}$$

[see Eqs. (3.12) in which $K_+ = K_-{}^*$ and $p = 0$]. While $|\psi_{NC}(0)\rangle$ is perfectly stable, $|\psi_C(0)\rangle$ is not, since it may get excited through interaction with the lasers at a rate Γ' [Eq. 3.15]. After a time long compared with Γ'^{-1}, the atom will either be in $|\psi_{NC}(0)\rangle$, where it will remain trapped, or it will be involved in some new fluorescence cycles. This filtering process thus leaves 50% of the atoms in the trapping state $|\psi_{NC}(0)\rangle$, while the other 50% resume a sequence of fluorescence cycles. The physical mechanism involved in this filtering is the Raman interaction that builds up the coherence between $|g_-, -\hbar k\rangle$ and $|g_+, +\hbar k\rangle$ that is characteristic of $|\psi_{NC}(0)\rangle$.

The reason why $|\psi_{CN}(0)\rangle$ cannot be directly populated from $|e_0, p\rangle$ by spontaneous emission is related to the conservation of linear momentum. Just after the spontaneous emission of a photon with momentum u, along Oz, an atom starting from $|e_0, p\rangle$ has its momentum changed from p to $p - u$. On the other hand, $|\psi_{NC}(0)\rangle$ is not an eigenstate of the atomic momentum P_{at}^z. It follows that the spontaneous emission of a photon with momentum u along Oz cannot connect $|e_0, p\rangle$ to both states $|g_+, +\hbar k\rangle$ and $|g_-, -\hbar k\rangle$.

One may wonder how to deal with linear-momentum conservation during the second step, i.e., during the filtering process. In fact, the laser fields have been considered here as external classical fields, and there is no isolated system in which one can look for momentum conservation. We could indeed generalize our treatment by quantizing the laser fields. In such a treatment, one finds that the three states of a given family have the same total linear momentum (sum of the atomic and laser field linear momentum) equal to the label p of the family, modulo $\hbar k$. The filtering process, leading from $|g_-, -\hbar k\rangle$ with the laser field in a certain quantum state to $|\psi_{NC}(0)\rangle$ with the laser field in a different state, conserves the total linear momentum.

5. EVOLUTION OF THE ATOMIC MOMENTUM DISTRIBUTION

A. Initial State

For the initial atomic state, we take a statistical mixture of the two ground states g_+ and g_- with the same momentum distribution along Oz:

$$\mathcal{P}_+{}^0(p_{at}^z) = \mathcal{P}_-{}^0(p_{at}^z). \tag{5.1}$$

The initial density matrix elements are thus equal to zero, except for σ_{++} and σ_{--}:

$$\begin{aligned} \sigma_{++}(p) &= \mathcal{P}_+{}^0(p + \hbar k), \\ \sigma_{--}(p) &= \mathcal{P}_-{}^0(p - \hbar k), \\ \sigma_{ee}(p) &= 0, \\ \sigma_{+-}(p) &= \sigma_{e+}(p) = \sigma_{e-}(p) = 0. \end{aligned} \tag{5.2}$$

The assumption that there are no coherences and that the momentum distributions are the same in the two ground-state sublevels is quite natural for atoms in an atomic beam emerging from a nozzle. However, in the real experiment[4] there is also an initial population in the $m = 0$ ground sublevel that will be optically pumped into g_+ and g_-; in some circumstances (laser detuning different from 0) the resulting distributions may be dissymmetric, and condition (5.1) may not be fulfilled in some experiments. However, we keep such a condition in the subsequent calculation since it allows us to extract simply the most important features of the new cooling process.

B. Master Equation: Generalized Optical Bloch Equations

Adding the terms found in Section 3 and Subsection 4.B, we get the equations governing the evolution of the density-matrix elements:

$$\frac{d\sigma}{dt} = \left(\frac{d\sigma}{dt}\right)_{Ham} + \left(\frac{d\sigma}{dt}\right)_{sp}, \tag{5.3}$$

where the first term [Eqs. (3.11)] is the Hamiltonian evolution corresponding to free evolution and atom–laser coupling. The second term [Eqs. (4.2) and (4.3)] corresponds to spontaneous emission.

In spite of the fact that internal and external degrees of freedom are treated completely quantum mechanically, this set of equation is remarkably simple, and it is well adapted for a numerical step-by-step time integration. Note in particular that the finite momentum exchange $\hbar k$ (recoil) is accounted for in all atom–field interactions, although it does not appear explicitly in the atom–laser interaction because of the concise notations [Eqs.(3.2)].

C. Final Atomic Distribution

We are interested in the atomic linear-momentum distribution along Oz at the end of the interaction with the lasers, whatever the internal state of the atoms may be. This distribution is[19]

$$\mathcal{P}(p_{at}^z) = \sigma_{++}(p_{at}^z - \hbar k) + \sigma_{--}(p_{at}^z + \hbar k) + \sigma_{ee}(p_{at}^z). \tag{5.4}$$

We can predict the shape of this distribution by using the results of Sections 3 and 4. Velocity-selective coherent population trapping consists in accumulating atoms around the trapping state:

$$|\psi_{NC}(0)\rangle = \frac{1}{\sqrt{2}} [|g_-, -\hbar k\rangle - |g_+, +\hbar k\rangle] \tag{5.5}$$

[see Eq. (3.12a) with $K_+ = K_-$ and $p = 0$].

First consider atoms trapped in $|\psi_{NC}(0)\rangle$. This state is not an eigenstate of the linear-momentum operator, and a linear-momentum measurement will yield either $p_{at}^z = +\hbar k$ or $p_{at}^z = -\hbar k$ with equal probability (case $|K_+| = |K_-|$). The corresponding atomic-momentum distribution $\mathcal{P}(p_{at}^z)$ is a double Dirac peak at $\pm\hbar k$ [solid vertical lines of Fig. 4(a)]. For such atoms, the distribution of the population of the noncoupled states $\langle\psi_{NC}(p)|\sigma|\psi_{NC}(p)\rangle$ is a single Dirac peak at $p = 0$ [solid vertical line of Fig. 4(b)].

Now consider atoms in $|\psi_{NC}(p)\rangle$ with p close to 0. Their atomic-momentum distribution $\mathcal{P}(p_{at}^z)$ is a shifted double Dirac peak at $p_{at}^z = p \pm \hbar k$ [dashed vertical lines of Fig. 4(a)]. The corresponding distribution of $|\psi_{NC}(p)\rangle$ exhibits a single Dirac peak with the same shift [dashed vertical line of Fig. 4(b)].

We can then predict the atomic-momentum distribution

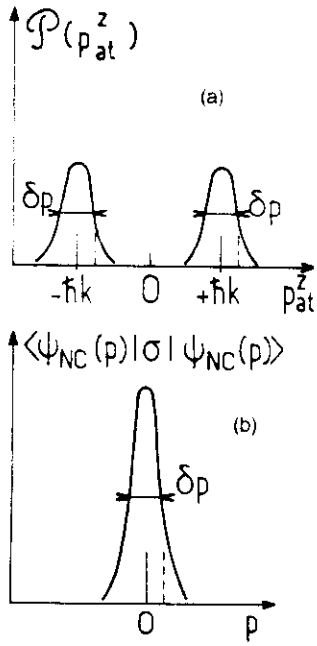

Fig. 4. Expected shape (a) of the atomic-momentum distribution $\mathcal{P}(p_{at}^z)$ and (b) of the population in the noncoupled state $\langle\psi_{NC}(p)|\sigma|\psi_{NC}(p)\rangle$. The vertical solid lines indicate the positions of the Dirac functions representing the contribution of the atoms in $|\psi_{NC}(0)\rangle$. The dashed vertical lines indicate the positions of the Dirac functions representing the contribution of atoms in $|\psi_{NC}(p)\rangle$. For atoms accumulated in noncoupled states $|\psi_{NC}(p)\rangle$ with p in a narrow range δp around $p = 0$ (b), the expected atomic-momentum distribution consists of twin peaks centered at $\pm\hbar k$, with the same shape and the same width δp (a).

after an interaction time θ. As a consequence of inequality (3.17), atoms are accumulated in states $|\psi_{NC}(p)\rangle$ with p in a narrow band around $p = 0$ with a width δp of the order of

$$\delta p \simeq \frac{M}{k\sqrt{\Gamma}}\frac{K}{\sqrt{\theta}}. \tag{5.6}$$

The corresponding atomic-momentum distribution $\mathcal{P}(p_{at}^z)$ will thus exhibit two peaks of width δp around $p_{at}^z = \pm\hbar k$ [Fig. 4(a)]. Finally, these two peaks will emerge over a broad background corresponding to atoms in the states $|\psi_C(p)\rangle$.

6. NUMERICAL ANALYSIS AND DISCUSSION OF THE RESULTS

We have obtained numerical solutions of the generalized optical Bloch equations with internal and external degrees of freedom [Eq. (5.3)], making use of the convenient p family basis introduced above. We have used the parameters corresponding to the experiment[4] on the transition $2\,^3S_1$–$2\,^3P_1$ at $\lambda = 1.083\ \mu$m of ^{4}He atoms ($\Gamma/2\pi = 1.6$ MHz).

A. Numerical Procedure

The time evolution of the density-matrix elements is obtained by incrementation starting from the initial condition of Eq. (5.1). The time increment is typically $0.05\ \Gamma^{-1}$, small enough to have no artificial instabilities introduced by the incrementation.

The p variable is discretized in intervals $\epsilon = \hbar k/30$, between $-p_{max}$ and $+p_{max}$ (typically $p_{max} = 30\ \hbar k$). These values have been chosen in order to fulfill the following requirements: First, ϵ must be small compared with the narrowest structure appearing in the p dependence of the solution of Eq. (5.3). Second, p_{max} must be large enough that the interesting part of the solution (near $p = 0$) is not affected by the truncation of the p range. We have chosen $p_{max} = 30\hbar k$ so that, for the largest value of θ considered here ($\theta = 1000\Gamma^{-1}$), the effect of momentum diffusion from p values larger than p_{max} to $p = 0$ is negligible.

B. Time Evolution of the Momentum Distribution

Figure 5 represents the final atomic-momentum distribution $\mathcal{P}(p_{at}^z)$ for four different interaction times ($\theta\Gamma = 50, 150, 400, 1000$). We have taken a zero detuning ($\delta_L = \omega_L - \omega_0 = 0$), a Rabi frequency $K = |K_+| = |K_-| = 0.3\Gamma$, and a Gaussian initial distribution with a standard half-width at $\exp(-1/2)$: $\Delta p_0 = 3\hbar k$. For θ large enough, $\mathcal{P}(p_{at}^z)$ exhibits two resolved peaks emerging at $\pm\hbar k$ above the initial distribution. This is the signature of the new cooling scheme. It is remarkable that, for $\theta = 150\ \Gamma^{-1}$, the cooling effect already appears. When the interaction time increases, the two peaks become narrower and higher.

Figure 6 shows on a larger momentum interval the shape of the right wing of $\mathcal{P}(p_{at}^z)$ (the curve is symmetrical) at the initial and final times. Besides the cooling effect, one sees that a fraction of atoms has diffused toward higher momentum values, which is in agreement with the physical picture of a diffusion in momentum space produced by spontaneous emission.

In order to visualize the accumulation of atoms in $|\psi_{NC}(p)\rangle$ with p close to 0, we have also calculated the populations $\langle\psi_{NC}(p)|\sigma|\psi_{NC}(p)\rangle$ and $\langle\psi_C(p)|\sigma|\psi_C(p)\rangle$. Figure 7 shows the

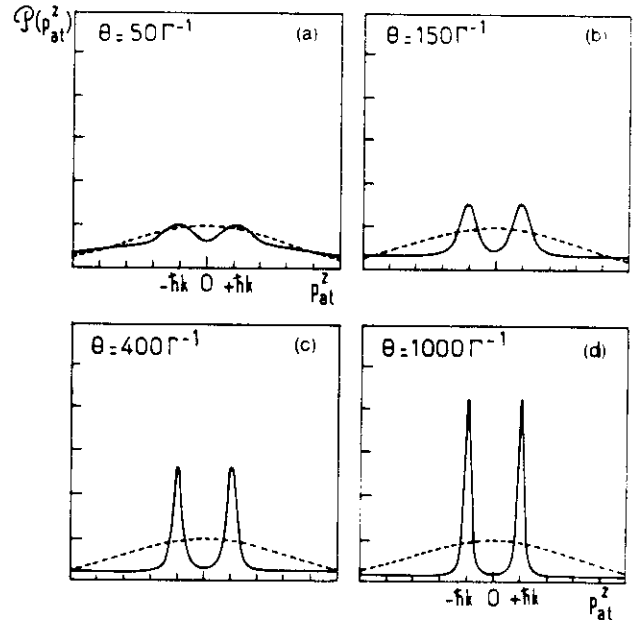

Fig. 5. Time evolution of the atomic-momentum distribution $\mathcal{P}(p_{at}^z)$. The dashed curves with half-width $\Delta p_0 = 3\hbar k$ show the initial distribution. As the interaction time θ increases, the height of the double peak at $\pm\hbar k$ (characterizing the new cooling process) increases, and its width decreases. Conditions for these figures: laser detuning $\delta_L = 0$; Rabi frequencies of the atom laser coupling $|K_+| = |K_-| = 0.3\Gamma$.

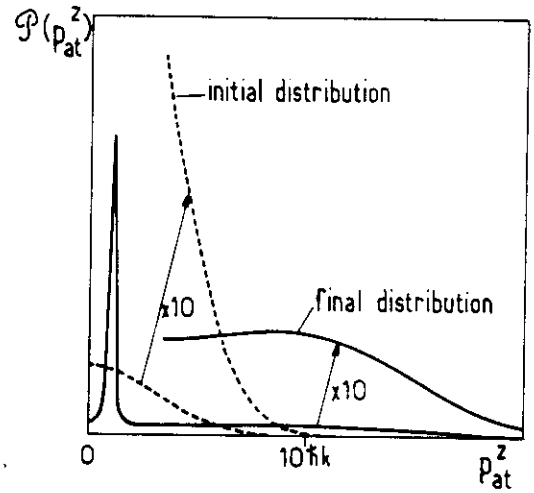

Fig. 6. Half of Fig. 5(d) with a different scale showing the diffusion of a fraction of the atoms toward large values of the momentum.

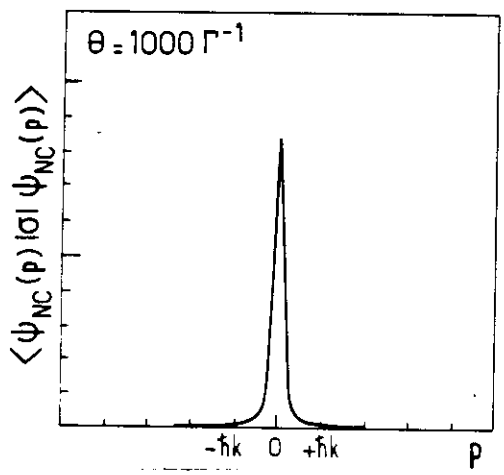

Fig. 7. Atomic population in the noncoupled states $|\psi_{NC}(p)\rangle$ in the same situation as for Fig. 5(d). The peak height is twice as large, and the width is the same as in one peak of Fig. 5(d). At this scale, the population in $|\psi_C(p)\rangle$ would not be visible.

resulting distribution of $\langle\psi_{NC}(p)|\sigma|\psi_{NC}(p)\rangle$ for the same parameters as in Fig. 5(d) [at this scale, $\langle\psi_C(p)|\sigma|\psi_C(p)\rangle$ is so small that it would not be visible]. The sharp peak near $p = 0$ appearing in the $|\psi_{NC}(p)\rangle$ population is clearly related to the double peak with the same width in the atomic-momentum distribution. The big difference between $\langle\psi_{NC}(p)|\sigma|\psi_{NC}(p)\rangle$ and $\langle\psi_C(p)|\sigma|\psi_C(p)\rangle$ near $p = 0$ shows that the coherence between $|\psi_{NC}(p)\rangle$ and $|\psi_C(p)\rangle$ is very small. In such a situation, the atomic distribution in the peaks can be considered a statistical mixture of $|\psi_{NC}(p)\rangle$ and $|\psi_C(p)\rangle$. We have checked that, outside the peak of Fig. 7, of the populations $\rangle$ and $|\psi_C(p)\psi_{NC}(p)\rangle$ are almost equal.

C. Peak Width, Temperature

In order to characterize the cooling process, we define a temperature in terms of the width of a momentum distribution. According to the discussions above, the cooled atoms are in states $|\psi_{NC}(p)\rangle$ with a distribution of p values shown in Fig. 7. We use the width of this distribution, which is also the width of each of the two peaks of Fig. 5(d), to define a temperature. Since we do not address the question of a Gaussian shape for this distribution, we will not give a precise value for the temperature. We can nevertheless note that the peak half-width may become much smaller than the one-photon recoil, corresponding to a temperature below the recoil energy.

We have plotted the half-width Δp [taken arbitrarily at $\exp(-1/2)$ after subtraction of the broad background] as a function of the interaction time θ [Fig. 8(a)] and of the Rabi frequency K [Fig. 8(b)]. The results obtained are in good agreement with a simple model based on relation (5.6), which predicts a width varying as $K\theta^{-1/2}$.

Remark

To characterize the temperature, one could also calculate the mean kinetic energy of the momentum distribution. We do not think that such a quantity would be appropriate for defining a temperature since, even if all atoms were in the pure state $|\psi_{NC}(0)\rangle$, their kinetic energy would be nonzero and equal to the recoil energy E_R, although this situation obviously corresponds to a zero temperature.

D. Unbalanced Laser Beams

Figure 9 shows the atomic-momentum distribution for unequal Rabi frequencies ($K_+ = 1.5K_-$). The peak height difference is easily interpreted: when $K_+ \neq K_-$, the coefficients of the expansion of the trapping state $|\psi_{NC}(0)\rangle$ on $|g_+, +\hbar k\rangle$ and $|g-, -\hbar k\rangle$ [Eq. (3.12a)] have different moduli.

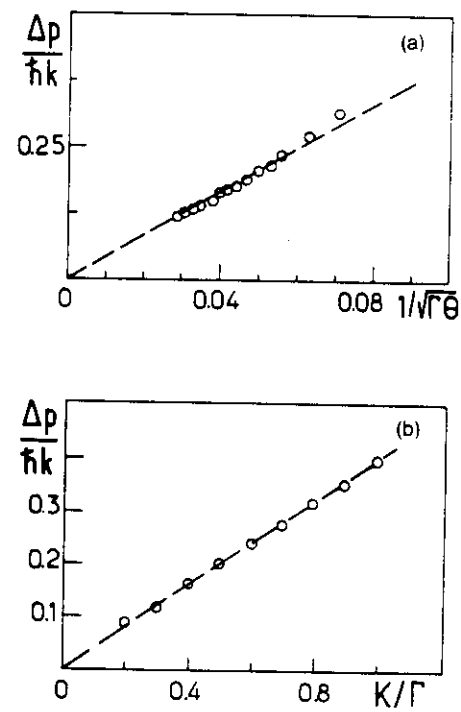

Fig. 8. Half-width of the peaks (initial half-width $\Delta p_0 = 3\hbar k$, laser detuning $\delta_L = 0$): (a) Δp for various interaction times θ for a Rabi frequency $K = 0.3\Gamma$; (b) Δp as a function of the Rabi frequency $K = K_+ = K_-$ for an interaction time $\theta = 1000\Gamma^{-1}$. These results show that Δp in proportional to $\theta^{-1/2}$ and to K (dashed lines) and thus confirm relation (5.6) for θ large enough that the two peaks are well separated.

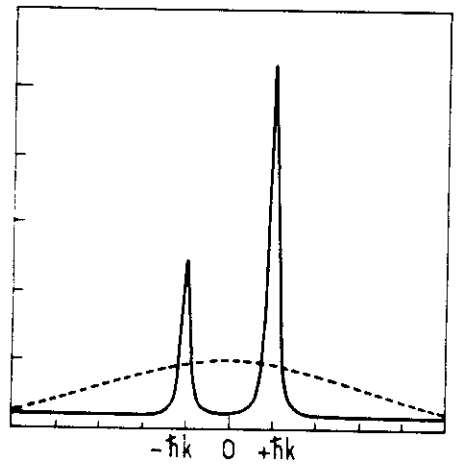

Fig. 9. Atomic-momentum distribution for unbalanced laser beams. Same conditions as for Fig. 5(d) except for the Rabi frequencies: $K_+ = 0.3\Gamma$; $K_- = 0.2\Gamma$.

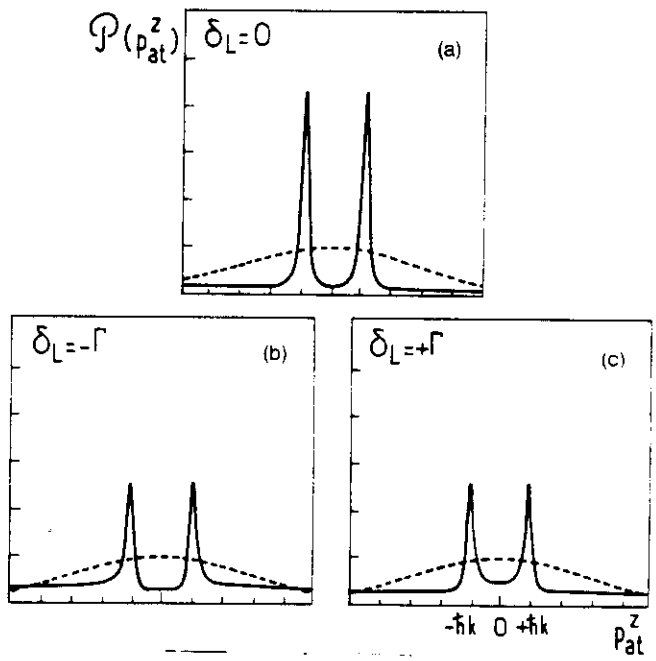

Fig. 10. Atomic-momentum distribution for various detunings. Same conditions as for Fig. 5(d) except for the detunings δ_L $\pm\Gamma$ (a), corresponding to $\delta_L = 0$, is the same as Fig. 5(d)]. Cooling is efficient for any sign of the detuning.

One predicts that for atoms trapped in $|\psi_{NC}(0)\rangle$ the probability for a momentum $+\hbar k$ is $|K_+/K_-|^2$ times greater than the probability for $-\hbar k$. This is in good agreement with the ratio of the two peaks of Fig. 9, which is found equal to 2.25 (theoretical value, 9/4).

E. Dependence on Laser Detuning

Figure 10 shows the atomic distribution at a given interaction time $\theta = 1000\Gamma^{-1}$ for three different laser detunings ($\delta_L = 0$, $\delta_L = \pm\Gamma$) and for the same laser intensities ($K_+ = K_- = K$). Note first that the new cooling mechanism is efficient for the three values of the detuning and particularly that it does not depend strongly on the sign of δ_L. This has to be contrasted with other schemes such as Doppler cooling, stimulated molasses, and polarization gradient cooling, which have a dispersionlike behavior.

The variation with δ_L of the height and width of the peaks can be interpreted by an extension of the perturbative calculation of Remark (i), Subsection 3.C, to a nonzero detuning. In this case, the width Γ' of $|\psi_C(p)\rangle$ is changed [from Eq. (3.15)] to

$$\Gamma' = (K^2/2)\frac{\Gamma}{\delta_L^2 + \frac{\Gamma^2}{4}}. \tag{6.1}$$

In addition, $|\psi_C(p)\rangle$ undergoes a light shift[20]

$$\delta' = (K^2/2)\frac{\delta_L}{\delta_L^2 + \frac{\Gamma^2}{4}}. \tag{6.2}$$

With these modifications taken into account, the motional coupling kp/M between $|\psi_{NC}(p)\rangle$ and $|\psi_C(p)\rangle$ now gives to $|\psi_{NC}(p)\rangle$ a width Γ'':

$$\Gamma'' = (kp/M)^2\frac{\Gamma'}{\delta'^2 + \frac{\Gamma'^2}{4}}. \tag{6.3}$$

Inserting Eqs. (6.1) and (6.2) into Eq. (6.3), we find that

$$\Gamma'' = (kp/M)^2\frac{\Gamma}{K^2/2}, \tag{6.4}$$

which coincides with Eq. (3.16), showing that Γ'' does not depend on the detuning δ_L. This explains why the peak width, which is determined by Γ'' [Remark (i) of Subsection 3.C], keeps the same value for the three curves of Fig. 10. On the other hand, Eq. (6.1) shows that Γ' decreases when the detuning increases: the absorption rate for atoms in $|\psi_C(p)\rangle$ is then weaker, yielding a lower optical pumping rate into $|\psi_{NC}(0)\rangle$. This explains the smaller peak heights in Figs. 10(b) and 10(c).

Note finally that there are small differences between the curves corresponding to $\delta_L = +\Gamma$ and $\delta_L = -\Gamma$. These differences have not yet been interpreted.

F. Efficiency of the Cooling Process

The cooling process is characterized not only by its ability to yield atoms in a narrow p range but also by the accumulation of atoms in this range, leading to a final density (in p space) larger than the initial one. The density at the center of the cooled distribution (near $p = 0$) is measured by the peak height.

We first considered the case of narrow initial distributions centered on $p = 0$. Figure 11(a) shows the evolution of the peak height as a function of the interaction time for an initial width of the momentum distribution $\Delta p_0 = \hbar k$. We have checked that, for the same total number of atoms, the evolution is almost independent of the width of the initial distribution, provided that this width is smaller than $2\hbar k$. An immediate interpretation is that each fluorescence cycle produces a redistribution in p space over an interval $2\hbar k$. After a few fluorescence cycles, there is no memory of structures narrower than $2\hbar k$. In agreement with the interpretation of this new cooling scheme, the peak height increases

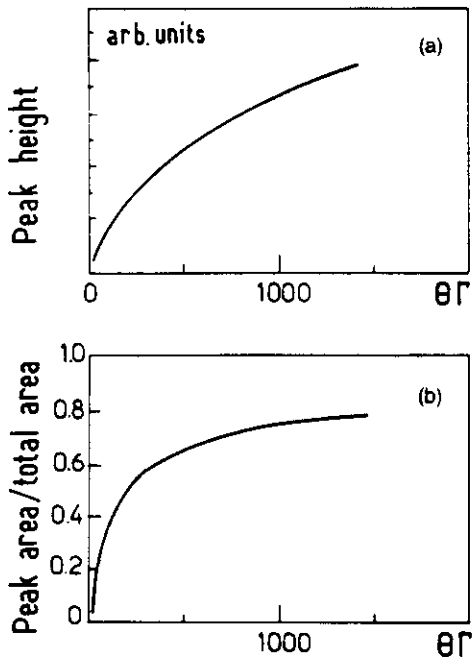

Fig. 11. Accumulation of atoms in the peaks as a function of time. The height of the peak (a) is a measure of the maximum atomic density in the p space. (b) Shows the fraction of atoms in the peaks. Conditions are the same as for Fig. 5 except for the initial distribution ($\Delta p_0 = \hbar k$).

with time. The decrease of the slope can be related to a depletion of the background of untrapped atoms that constitute a reservoir for the accumulation process. It is also interesting to study the evolution of the total number of atoms in the peaks, since this results from opposite variations of height (which increases) and of the width (which decreases). Figure 11(b) shows that a large fractions of the atoms can be trapped in the peaks of cooled atoms.

We also investigated the case of broad initial distribution ($\Delta p_0 > 3\hbar k$). For small interaction times θ, the evolution of the peak height versus θ is linear and depends only on the initial atomic density at $p = 0$. But a decrease of the slope appears at an interaction time that is longer when the initial distribution is broader. As a consequence, the peak height (normalized by the initial density at $p = 0$) is larger for broader initial distribution when θ is long enough. For example, for $\Delta p_0 = 10\,\hbar k$ and $\theta = 1000\Gamma^{-1}$ the normalized peak height is 1.7 times larger than the one of Fig. 5(d) (corresponding to $\Delta p_0 = 3\hbar k$, $\theta = 1000\Gamma^{-1}$). This behavior can be interpreted by considering the diffusion of atoms in momentum space, from the edges of the initial distribution to $p = 0$, where they can be trapped. Note finally that for Δp_0 large enough (and for $\delta_L = 0$) the Doppler detuning can decrease the diffusion rate at the edges of the momentum distribution, which introduces a natural cutoff that is independent of Δp_0.

This discussion clearly raises the question of the asymptotic behavior at long interaction times. One can hardly rely on a numerical calculations to answer this question. Note that a double Dirac peak (corresponding to $|\psi_{NC}(0)\rangle$) is a steady-state solution of Eq. (5.3), but we do not know whether such a solution can be reached by starting from realistic initial conditions. This question is still unresolved.

In order to increase the fraction of cooled atoms, we have considered schemes in which atoms with large p would be reflected toward $p = 0$ by interaction with another laser beam. With such walls in p space, it is clear that the accumulation process into $|\psi_{NC}(0)\rangle$ will continue indefinitely.

7. GENERALIZATION TO TWO DIMENSIONS

So far we have dealt only with one-dimensional cooling. Now we explain how velocity-selective coherent population trapping can be extended to two dimensions. We consider the same atomic transition $J_g = 1 \leftrightarrow J_e = 1$ as the one used in the experimental demonstration of one-dimensional cooling.[4] Figure 12(a) represents the various Zeeman sublevels in the ground state and in the excited state and the Clebsch–Gordan coefficients of the various transitions $g_m \leftrightarrow e_{m'}$ (m, $m' = -1, 0, +1$). The laser configuration consists of three laser beams [Fig. 12(b)] with the same frequency and the same amplitude. As above, there are two counterpropagating beams along Oz, one σ_+ polarized with a wave vector $k\hat{e}_z$ one σ_- polarized with a wave vector $-k\hat{e}_z$ (k is the wave number; $\hat{e}_z$ is a unit vector along Oz). In addition, there is a third laser beam along Ox (wave vector $k\hat{e}_x$), linearly polarized along Oz (π polarization). Each of these beams excites only one type of transition: $g_m \leftrightarrow e_{m+1}$ for the σ_+ beam, $g_m \leftrightarrow e_{m-1}$ for the σ_- beam, and $g_m \leftrightarrow e_m$ for the π beam.

Consider the state

$$|\psi_{NC}(\mathbf{p})\rangle = \frac{1}{\sqrt{3}}\left(|g_{-1}, \mathbf{p} - \hbar k\hat{e}_z\rangle + |g_0, \mathbf{p} + \hbar k\hat{e}_x\rangle + |g_{+1}, \mathbf{p} + \hbar k\hat{e}_z\rangle\right), \quad (7.1)$$

which is a linear superposition of three states differing not

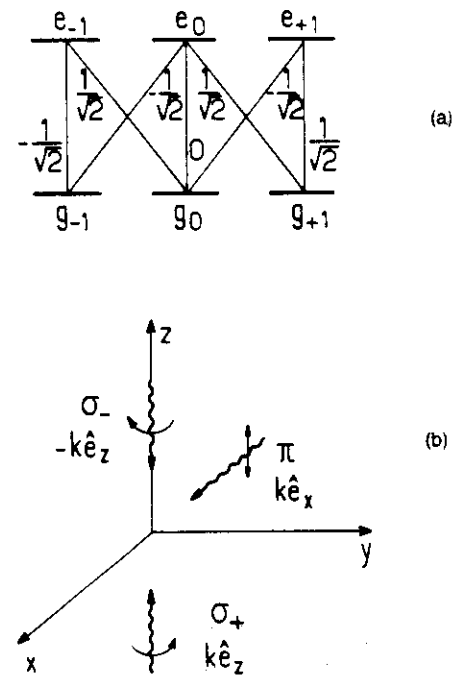

Fig. 12. Configuration for two-dimensional velocity-selective coherent population trapping. (a) The $J = 1 \leftrightarrow J = 1$ atomic transition with the corresponding Clebsch–Gordan coefficients. (b) The three laser wave vectors and polarizations for which the state defined in Eq. (7.1) is trapping and velocity selective along Ox and Oz.

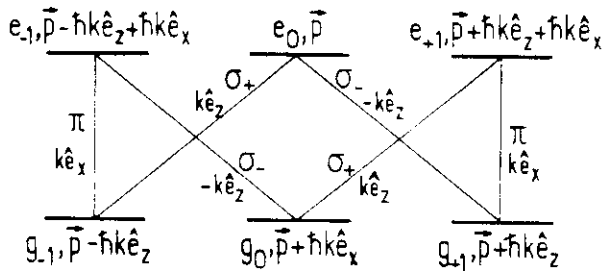

Fig. 13. Closed family of states coupled by interaction with the lasers of Fig. 12(b). Each state is characterized by its internal and external quantum numbers.

only in their internal quantum numbers but also in their momenta. We are going to show that such a state cannot be coupled to any excited state in the same way as the $|\psi_{NC}(p)\rangle$ states introduced in Subsection 3.C. For that purpose we first determine to what excited states each component of Eq. (7.1) is coupled (Fig. 13). Because of the conservation of angular and linear momentum, an atom in $|g_{-1}, \mathbf{p} - \hbar k\hat{e}_z\rangle$ is coupled only to $|e_{-1}, \mathbf{p} - \hbar k\hat{e}_z + \hbar k\hat{e}_x\rangle$ by absorption of a $(\pi, k\hat{e}_x)$ photon and to $|e_0, \mathbf{p}\rangle$ by absorption of a $(\sigma_+, k\hat{e}_z)$ photon. In the same way, $|g_0, \mathbf{p} + \hbar k\hat{e}_x\rangle$ is coupled only to $|e_{-1}, \mathbf{p} - \hbar k\hat{e}_z + \hbar k\hat{e}_x\rangle$ (respectively, $|e_{+1}, \mathbf{p} + \hbar k\hat{e}_z + \hbar k\hat{e}_x\rangle$) by absorption of a $(\sigma_-, -k\hat{e}_z)$ [respectively, $(\sigma_+, k\hat{e}_z)$] photon, and $|g_{+1}, \mathbf{p} + \hbar k\hat{e}_z\rangle$ is coupled only to $|e_{+1}, \mathbf{p} + \hbar k\hat{e}_z + \hbar k\hat{e}_x\rangle$ (respectively, $|e_0, \mathbf{p}\rangle$) by absorption of a $(\pi, k\hat{e}_x)$ [respectively, $(\sigma_-, -k\hat{e}_z)$] photon. As in Section 3, we thus find a family of six states (instead of three) $\{|g_{-1}, \mathbf{p} - \hbar k\hat{e}_z\rangle, |g_0, \mathbf{p} + \hbar k\hat{e}_x\rangle, |g_{+1}, \mathbf{p} + \hbar k\hat{e}_z\rangle, |e_{-1}, \mathbf{p} - \hbar k\hat{e}_z + \hbar k\hat{e}_x\rangle, |e_0, \mathbf{p}\rangle, |e_{+1}, \mathbf{p} + \hbar k\hat{e}_z + \hbar k\hat{e}_x\rangle\}$ that remains closed with respect to absorption and stimulated-emission processes. The important point is that all transition amplitudes starting from Eq. (7.1) and ending in any of the three excited states of the family interfere destructively. This is because each of the three excited states of Fig. 13 is coupled only to two ground states (because of the zero value of the Clebsch–Gordan coefficient for $e_0 \leftrightarrow g_0$) by two transitions having opposite Clebsch–Gordan coefficients [Fig. 12(a)]. Since the state [Eq. (7.1)] is completely symmetric, the six excitation amplitudes from such a state interfere destructively two by two.

Consequently, an atom in Eq. (7.1) cannot leave this state by interaction with the lasers. Since it contains only ground states, it cannot decay by spontaneous emission. It remains to see under what condition it is stationary with respect to the free evolution Hamiltonian H_A. We must write that the kinetic energies of the three components of Eq. (7.1) are the same (as above, we suppose that there is no static magnetic field), which gives

$$(\mathbf{p} - \hbar k\hat{e}_z)^2 = (\mathbf{p} + \hbar k\hat{e}_x)^2 = (\mathbf{p} + \hbar k\hat{e}_z)^2. \tag{7.2}$$

We conclude that $|\psi_{NC}(\mathbf{p})\rangle$ is a perfect trap only if

$$\mathbf{p} \cdot \hat{e}_z = \mathbf{p} \cdot \hat{e}_x = 0. \tag{7.3}$$

This shows that optical pumping into the states [Eq. (7.1)] satisfying Eq. (7.3) could provide a two-dimensional cooling for the components of $\mathbf{p}$ perpendicular to $\hat{e}_y$.

Experimentally, one could send an atomic beam along Oy in the laser configuration of Fig. 12(b). Accumulation of atoms by optical pumping into the trapping states Eq. (7.1) satisfying Eq. (7.3) could be revealed by measuring P_{at}^x and P_{at}^z after the interaction zone. From Eqs. (7.1) and (7.3) we then predict that the surface giving the atomic-momentum distribution in the (p_x, p_z) plane should exhibit three narrow peaks, at

$$\begin{cases} p_{at}^x = 0 \\ p_{at}^z = +\hbar k \end{cases}, \quad \begin{cases} p_{at}^x = 0 \\ p_{at}^z = -\hbar k \end{cases}, \quad \begin{cases} p_{at}^x = +\hbar k \\ p_{at}^z = 0 \end{cases}. \tag{7.4}$$

Remark

Note that in such an experiment there must be no force acting along the velocity-selective directions Ox and Oz. In order to avoid the effect of gravity, we should thus align the atomic beam vertically.

In this section we have demonstrated that there is a perfect trapping state that is velocity selective in two dimensions. However, in order to evaluate the efficiency of the cooling process, one should also solve the generalized optical Bloch equations corresponding to this situation. This would allow one to evaluate how long it would take for momentum diffusion in two dimensions to accumulate many atoms into the trapping state.

It is tempting to try a further generalization to three dimensions. We have found no scheme that allows accumulation of many atoms into a noncoupled state that is velocity selective in three dimensions. We have found such states for more-complicated level schemes. Unfortunately, in the situations that we have investigated, there is always another trapping state that is velocity selective in a smaller number of dimensions (two or one). The atoms are then rapidly trapped into this less-selective noncoupled state, where they are no longer available for the three-dimensional trapping.

8. CONCLUSION

We have presented a full quantum theoretical treatment of a new one-dimensional laser-cooling scheme permitting transverse temperatures below the one-photon recoil energy to be reached by velocity-selective coherent population trapping. Unlike semiclassical approaches, this treatment can be applied to situations in which the atomic coherence length is comparable with or larger than the laser wavelength. It is based on the use of families that contain a finite number of states defined by translational and internal quantum numbers and that remain closed with respect to absorption and stimulated emission. Redistributions among these families occur through spontaneous emission. We have established generalized optical Bloch equations for the density-matrix elements corresponding to these families, and we have presented numerical solutions of these equations.

This theoretical study has allowed us to exhibit the essential features of the new cooling process and to support the underlying physical ideas. The main differences from other cooling methods are the following:

(i) The cooling exists for both signs of the detuning and for zero detuning;

(ii) The width of the final momentum distribution, which characterizes the temperature, decreases as $\theta^{-1/2}$, where θ is the interaction time. There is no fundamental

limit to the lowest temperature achievable by this method; in particular, the one-photon recoil is not a limit;

(iii) The basic cooling mechanism relies not on a friction force but on a diffusion process in momentum space, which pumps atoms into nonabsorbing states corresponding to a small region of the momentum space;

(iv) Since the cooled atoms no longer interact with the laser field they suffer no perturbation either on the external degrees of freedom (no diffusion) or on the internal degrees of freedom (no light shifts).

We presented in Section 7 a possible extension of this new cooling scheme to two dimensions. The method of families used in this paper could easily be applied to such a situation. It would also be interesting to add a supplementary interaction for reflecting toward $p = 0$ atoms that have diffused at large p values; such walls should improve the cooling efficiency at long interaction times.

The fundamental property on which the new cooling process is based is the quantum coherence between $|g_-, p - \hbar k\rangle$ and $|g_+, p + \hbar k\rangle$. A remarkable feature associated with this coherence is the total coherence between states of different linear momentum $p - \hbar k$ and $p + \hbar k$. Since p is distributed in a narrow interval around 0, such coherence gives rise to two coherent wave packets propagating along different directions. Another interesting feature is the complete correlation between the internal state and the direction of propagation, as in a Stern–Gerlach experiment. The calculations presented in this paper permit a quantitative treatment of all these coherence effects by use of the nondiagonal terms $\sigma_{+-}(p)$ of the density matrix. These results could be useful in the analysis of atomic interferences based on this scheme.

ACKNOWLEDGMENTS

We acknowledge many fruitful discussions with Jean Dalibard and Christophe Salomon. We thank F. Papoff for help with the numerical calculations. This research has been partly supported by the European Economic Community.

* Permanent address, Dipartimento di Fisica, Università di Pisa, I—56100 Pisa, Italy.

REFERENCES AND NOTES

1. P. D. Lett, R. N. Watts, C. I. Westbrook, W. D. Phillips, P. L. Gould, and H. J. Metcalf, Phys. Rev. Lett. **61**, 169 (1988).
2. J. Dalibard, C. Salomon, A. Aspect, E. Arimondo, R. Kaiser, N. Vansteenkiste, and C. Cohen-Tannoudji, in *Atomic Physics 11*, proceedings of the Eleventh International Conference on Atomic Physics, S. Haroche, J. C. Gay, and G. Grynberg, eds. (World Scientific, Singapore, 1989).
3. Y. Shevy, D. S. Weiss, and S. Chu, in *Proceedings of the Conference on Spin Polarized Quantum Systems*, S. Stringari, ed. (World Scientific, Singapore, 1989); see also Y. Shevy, D. S. Weiss, P. J. Ungar, and S. Chu, Phys. Rev. Lett. **62**, 1118 (1989).
4. A. Aspect, E. Arimondo, R. Kaiser, N. Vansteenkiste, and C. Cohen-Tannoudji, Phys. Rev. Lett. **61**, 826 (1988).
5. J. Dalibard and C. Cohen-Tannoudji, J. Opt. Soc. Am. B **6**, (1989).
6. Y. Castin, H. Wallis, and J. Dalibard, J. Opt. Soc. Am. B 6, (1989).
7. J. Dalibard and C. Cohen-Tannoudji, J. Phys. B 18, 1661 (1985), and references therein.
8. G. Alzetta, A. Gozzini, L. Moi, and G. Orriols, Nuovo Cimento **36B**, 5 (1976).
9. E. Arimondo and G. Orriols, Lett. Nuovo Cimento **17**, 333 (1976); H. R. Gray, R. W. Whitley, and C. R. Stroud, Opt. Lett. **3**, 218 (1978).
10. P. M. Radmore and P. L. Knight, J. Phys. B **15**, 561 (1982).
11. J. Dalibard, S. Reynaud, and C. Cohen-Tannoudji, in *Interaction of Radiation with Matter*, a volume in honour of Adriano Gozzini (Scuola Normale Superiore, Pisa, Italy, 1987), pp. 29–48.
12. V. G. Minogin and Yu. V. Rozhdestvenskii, Zh. Eksp. Teor. Fiz. **88**, 1950 (1985) [Sov. Phys. JETP **61**, 1156 (1985)]. The theoretical treatment of these authors is valid only for atomic momenta p larger than the photon momentum $\hbar k$ since their Fokker–Planck equation is based on an expansion in powers of $\hbar k/p$.
13. Other proposals for getting temperatures below the recoil limit have been presented. It has been suggested that optical pumping in translation space might be used to cool the translational degrees of freedom by velocity-selective recycling in a trap. See D. E. Pritchard, K. Helmerson, V. S. Bagnato, G. P. Lafyatis, and A. G. Martin, in *Laser Spectroscopy VIII*, S. Svanberg and W. Persson, eds. (Springer-Verlag, Heidelberg, 1987), p. 68.
14. Closed families exist only when the two counterpropagating waves have polarizations such that they cannot both excite the same atomic transition $|g, m\rangle \leftrightarrow |e, m'\rangle$. This is always the case for a $\sigma_+ - \sigma_-$ configuration because of angular-momentum conservation. In the particular cases of $J_g = 1 \leftrightarrow J_e = 0$ and $J_g = 1 \leftrightarrow J_e = 1$ transitions, closed families also exist when the two counterpropagating waves have orthogonal linear polarizations. This is easily seen by use of new bases of sublevels for g and e, such as $|g, m = 0\rangle$, $[|g, m = -1\rangle \pm |g, m = 1\rangle]/\sqrt{2}$. Using these new bases, we find that the two waves cannot excite the same transition. This explains why cooling by velocity-selective coherent population trapping has been also observed on the $2\,^3S_1$–$2\,^3P_1$ transition of ^{4}He with the orthogonal linear configuration.[4]
15. Ch. J. Bordé, in *Advances in Laser Spectroscopy*, F. T. Arrechi, F. Strumia, and H. Walther, eds. (Plenum, New York, 1983); S. Stenholm, Appl. Phys. **16**, 159 (1978).
16. R. J. Cook, Phys. Rev. A **22**, 1078 (1980).
17. C. Cohen-Tannoudji, in *Frontiers in Laser Spectroscopy*, R. Balian, S. Haroche, and S. Liberman, eds. (North-Holland, Amsterdam, 1977), p. 1. For an extension of these equations including translational quantum numbers, see S. Stenholm, Appl. Phys. **15**, 287 (1978).
18. In fact, the exact shape of $H(u)$ is not important, provided that it has the correct width $2\hbar k$ and it is normalized. We have checked that a constant value over $2\hbar k$ [$H(u) = 1/2\hbar k$ for $-\hbar k \leq u \leq \hbar k$] yields almost identical results after only a few fluorescence cycles. We have thus taken the constant form for $H(u)$, simpler for the calculations, for all the interaction times longer than $10\Gamma^{-1}$.
19. In an experiment like ours,[4] the atoms are allowed to fly a long distance without any interaction until they are detected. Excited atoms will then decay to one of the ground states, and the recoil of the corresponding photon has to be taken into account. The last term of Eq. (5.4) must then be convoluted by the kernel $H(u)$ introduced in Section 4. Note that this amounts to a convolution of $\sigma_{ee}(p)$ by a function with width $2\hbar k$. In the case of a high light intensity (for which our calculation is still valid), $\sigma_{ee}(p)$ assumes values comparable with those of $\sigma_{++}(p)$ or $\sigma_{--}(p)$, and this convolution will produce a widening of the narrow structures of $\sigma_{ee}(p)$. In the case of a weak intensity, this correction is negligible.
20. These results are readily obtained by following the method presented in C. Cohen-Tannoudji, Metrologia **13**, 161 (1977).